Precambrian Research 351 (2020) 105979

Contents lists available at ScienceDirect

Precambrian Research

journal homepage: www.elsevier.com/locate/precamres

Oceanic crust and mantle evidence for the evolution of Tonian-Cryogenian ophiolites, southern Brasiliano Orogen

M. Werle [a,*], L.A. Hartmann [a], G.N. Queiroga [b], C. Lana [b], J. Pertille [c], C.R.L. Michelin [a], M.V. D. Remus [a], M.P. Roberts [d], M.P. Castro [b], C.G. Leandro [a], J.F. Savian [a]

[a] Instituto de Geociências, Universidade Federal do Rio Grande do Sul, Avenida Bento Gonçalves, 9500, 91501-970 Porto Alegre, Rio Grande do Sul, Brazil
[b] Departamento de Geologia, Escola de Minas, Universidade Federal de Ouro Preto, Morro do Cruzeiro, 35400-000 Ouro Preto, Minas Gerais, Brazil
[c] Centro de Desenvolvimento Tecnológico, Universidade Federal de Pelotas, Pelotas, Brazil
[d] Centre for Microscopy Characterisation and Micro-Analysis, The University of Western Australia, Australia

ARTICLE INFO

Keywords:
Ophiolite
Metasomatic tourmaline
Mantle-derived Cr-spinel
B isotopes
Crustal evolution

ABSTRACT

Unravelling the complexity of tonian-cryogenian (950–680 Ma) evolution of ophiolites requires the search for rare mineral systems and their quantification with varied techniques. Ophiolites in the Brasiliano Orogen are widely distributed over 2,000 km along the eastern half of South America. We selected two ophiolites from different geotectonic settings of the Sul-Riograndense Shield, southern Brasiliano Orogen, to delimit the evolution of the oceanic phase of the orogen. The southern portion of the Bossoroca ophiolite is inserted in the São Gabriel juvenile terrane and contains rare metasomatic tourmaline in chloritite close to serpentinite and metamorphosed Cr-spinel. The southern Bossoroca ophiolite was intruded by Cerro da Cria and Ramada Granites and the U-Pb-Hf isotopic study of zircon from these rocks constrains the crustal evolution of the São Gabriel juvenile terrane. Capané ophiolite has similar age (793–715 Ma) as the Bossoroca ophiolite and was inserted in the Porongos fold-thrust belt with preserved Cr-spinel of mantellic composition. Integrated use of Cr-spinel mineral chemistry, B isotopes in tourmaline in the Bossoroca ophiolite and zircon U-Pb-Hf isotopes of granites associated with the southern Bossoroca ophiolite revealed several steps in the evolution of the ophiolites in the Dom Feliciano Belt. Capané Cr-spinel cores have mantle-derived compositions (Mg# 0.66 – 0.69; Cr# 0.51 – 0.53), tourmaline from the Bossoroca ophiolite is dravite and has $\delta^{11}B = 0$ to + 3, and granites crystallization ages are 578 ± 3.2 and 612 ± 12 Ma ($\varepsilon Hf_{zrn} = -10$ to −25). Zircon from other dravite occurrences of the Bossoroca ophiolite were previously dated at 920 Ma. We unraveled the main steps in the evolution of ophiolites from the southern Brasiliano Orogen, with emphasis on the Bossoroca and Capané ophiolites, during their trajectory from mid-ocean ridge (920 Ma), formation of dravite in oceanic crust, preservation of mantellic cores in Cr-spinel, and intrusion of craton-generated granites at 612–578 Ma.

1. Introduction

Ophiolites are associations of mafic, sedimentary and ultramafic rocks, remnants of oceanic crust and mantle associated with coeval metamorphic, sedimentary and igneous rocks that occur in orogenic belts and represent traces of ancient Wilson cycles (Dilek, 2003; Dilek and Furnes, 2014; Hartmann et al., 2019; Amaral et al., 2020). Ophiolites provide information about mid-ocean ridge and subduction zone processes, mantle dynamics, fluid-rock interactions and mechanisms of continental growth in accretionary and collisional belts (e.g., Saccani et al., 2020). Neoproterozoic ophiolites are present in the extensive (1000 km) Arabian-Nubian Shield of northeastern Africa and in South American terranes (Goiás – 500 km long, São Gabriel – 80 km) and are linked with the Brasiliano-Pan-African Orogeny (Dilek, 2003; Stern et al., 2004; Caxito et al., 2014; Azer, 2014; Brown et al., 2020). This orogeny was associated with the break-up of supercontinent Rodinia and later collage of West Gondwana (Suita et al., 2004; Brito-Neves et al., 2014; Hartmann et al., 2019). Tonian-cryogenian (950–680 Ma) ophiolites from the Dom Feliciano Belt, southern Brasiliano Orogen, are remnants of the Adamastor oceanic crust. In the São Gabriel juvenile terrane, western portion of the Dom Feliciano Belt, the remnants are associated with metaplutonic and metavolcanosedimentary rocks of

* Corresponding author.
E-mail address: marianawerle96@gmail.com (M. Werle).

https://doi.org/10.1016/j.precamres.2020.105979
Received 20 April 2020; Received in revised form 19 October 2020; Accepted 20 October 2020
Available online 29 October 2020

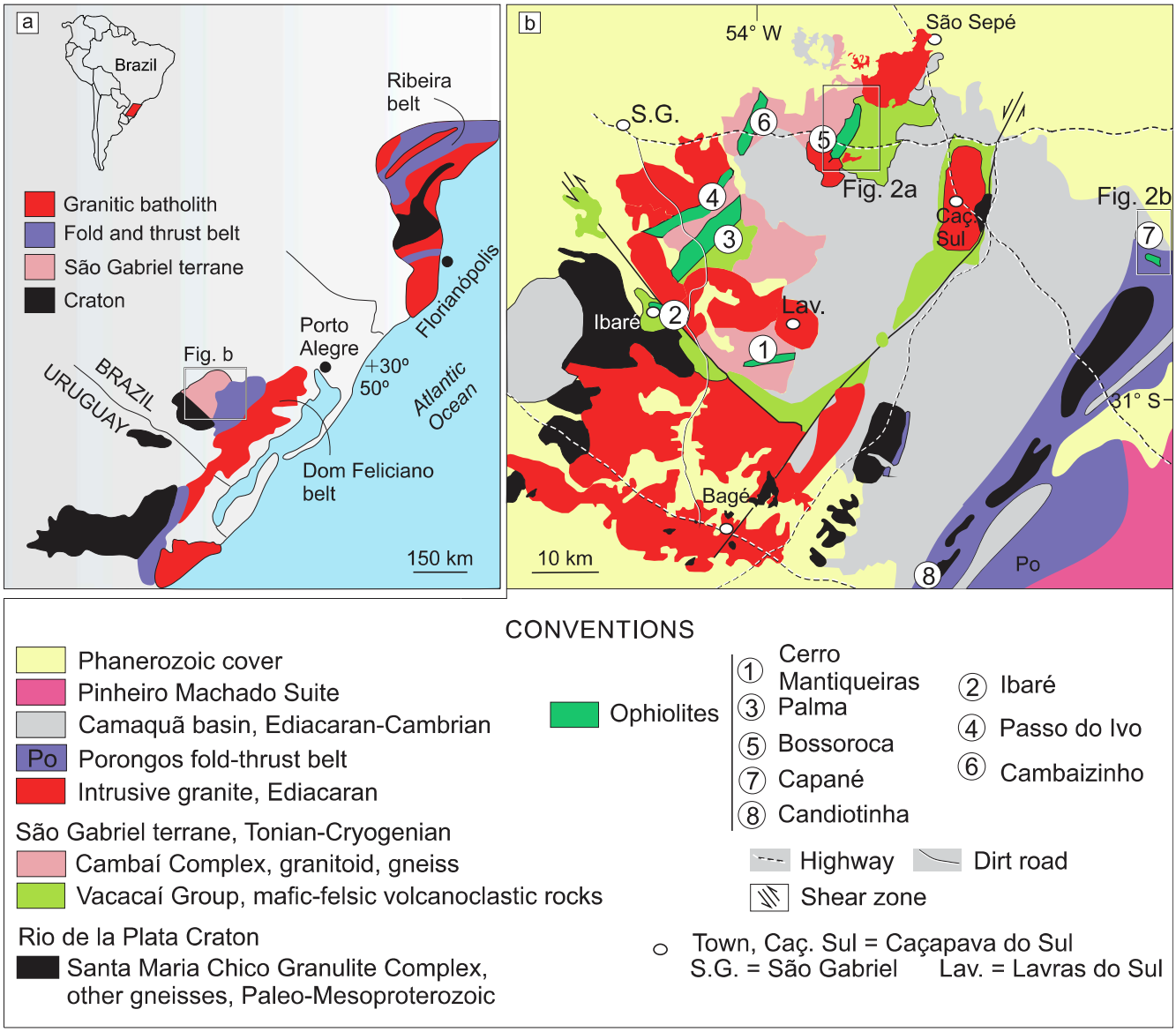

Fig. 1. (a) Geological map of the Dom Feliciano Belt (modified from Rapela et al., 2011; Arena et al., 2017; Hartmann et al., 2019). (b) Geological map of the Porongos fold-thrust belt, São Gabriel terrane and fragments of the Rio de La Plata craton, showing the location of ophiolites (1 to 7) (modified from Philipp et al., 2016; Hartmann et al., 2019; Cerva-Alves et al., 2020).

island arc environment (e.g., Cerro Mantiqueiras, Ibaré, Palma, Bossoroca and Cambaizinho ophiolites – (Hartmann and Chemale, 2003; Arena et al., 2016, 2017; Hartmann et al., 2019; Cerva-Alves et al., 2020). Ophiolite slices are also present in the central portion of the Dom Feliciano Belt associated with schists of the Porongos fold-thrust belt – Capané (Marques et al., 2003; Arena et al., 2018), Candiotinha (Xavier et al., 2019), Arroio Grande (Ramos et al., 2020) and correlative La Tuna (Uruguay; Peel et al., 2018).

Metasomatic mineral assemblages in ophiolite, in particular tourmaline associated with chloritite enclosed in serpentinite, help decipher the evolution of ultramafic rocks in oceanic crust environments. Cr-spinel is a main mineral in podiform chromitites (e.g., Abdel-Karim et al., 2018; Qiu and Zhu, 2018; Derbyshire et al., 2019; Hodel et al., 2019). Chromite indicates the mantle component of the ophiolite sequence (Arai and Miura, 2015). The only Cr-spinel with mantle-like composition in the Brasiliano Orogen was described in the Araguaia Belt (Kotschoubey et al., 2005; Hodel et al., 2019)). Despite accurate characterization of ophiolites in the Dom Feliciano Belt (e.g. Arena et al., 2016, 2017, 2018, 2020; Ramos et al., 2020; Hartmann et al., 2019), recent studies question the presence of oceanic crust in the Brasiliano Orogen (e.g., Konopásek et al., 2020), requiring additional characterization and evaluation of origin and evolution of the ophiolites. Accordingly, we studied mantellic Cr-spinel and dravite from the ophiolites; we added U-Pb-Hf isotopes in zircon from intrusive granites to constrain the final evolutionary stage of the terrane.

The objective is to describe the evolution of the Bossoroca and Capané ophiolites from the oceanic, accretionary phase of the Brasiliano Orogen. We studied petrography and mineral chemistry of serpentinite and chloritite samples from the two ophiolites. We focused on Cr-spinel and tourmaline mineral chemistry, B isotopes in tourmaline from the Bossoroca ophiolite and zircon U-Pb-Hf isotopes of two intrusions, Cerro da Cria and Ramada Granites, in the southern portion of the Bossoroca ophiolite. In addition, we report the chemical composition of mantle-derived Cr-spinel from the Capané ophiolite. The study of the Bossoroca and Capané ophiolites integrated with U-Pb dating and Lu-Hf isotopes in zircon of two intrusive granites in the Bossoroca ophiolite is key to understanding the evolution of the oceanic crust, mantle and continental crust in the Brasiliano Orogen.

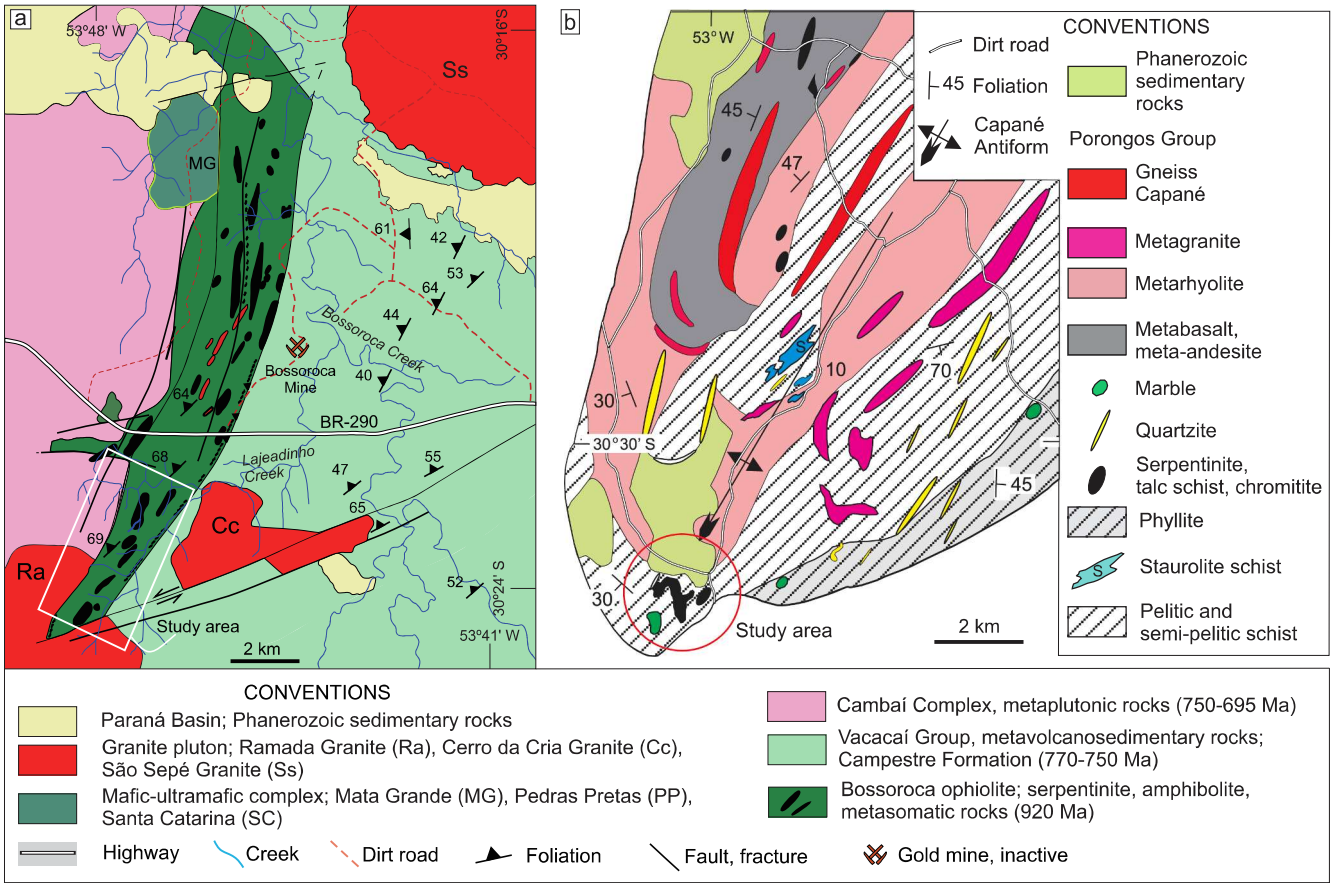

Fig. 2. (a) Geological map of Bossoroca ophiolite (modified from Gubert et al., 2016 and Massuda et al., 2020). (b) Geological map of Capané Antiform, Porongos Group (modified from Zvirtes et al., 2017).

2. Geological setting

The studied rock association is part of the extensive Neoproterozoic orogenic belt that extends along the eastern half of South America. Most of the Brasiliano Orogen was formed by continental collisional processes (660–500 Ma), but the São Gabriel terrane formed during the oceanic, accretionary stage (950–660 Ma) of the orogen. The terrane is part of the local Dom Feliciano Belt.

The Dom Feliciano Belt is the southern extension of the Neoproterozoic-Cambrian Brasiliano Orogen. The belt was formed by the collision of oceanic domains and continental fragments between the Rio de La Plata, Congo and Kalahari cratons during the formation of West Gondwana (Fernandes et al., 1992; Silva et al., 2005; Saalmann et al., 2011; Philipp et al., 2016). This orogenic belt extends from southern Uruguay to Santa Catarina state (Brazil) (Fig. 1a). The Sul-Riograndense Shield is located in the center of the Dom Feliciano Belt (Fig. 1b) and divided (from W to E) into: (1) Taquarembó terrane with Archean and Paleoproterozoic rocks interpreted as a fragment of the Rio de La Plata craton, (2) São Gabriel terrane as an association of juvenile magmatic arcs, (3) Porongos fold-thrust belt with metavolcanosedimentary rocks and inliers of basement rocks, (4) granitic rocks of Pelotas batholith and (5) foreland Camaquã Basin (Hartmann et al., 1999; Babinski et al., 1996; Saalmann et al., 2005; Pertille et al., 2017; Philipp and Machado, 2005; Paim et al., 2014).

The São Gabriel terrane is the western portion of the Dom Feliciano Belt and records the initial stages of the Brasiliano Orogen (Hueck et al., 2018). The terrane contains ophiolites (Arena et al., 2016), oceanic arc associations (Saalmann et al., 2007), late-tectonic basins (Cerva-Alves et al., 2020) and was pierced by post-tectonic granites (Chemale et al., 2000). The ophiolites are the oldest portion of the São Gabriel terrane. The mafic, ultramafic and metasomatic rocks that are remnants of the proto-Adamastor oceanic crust formed at ca. 920 Ma (Arena et al., 2016; Hartmann et al., 2019) between the Rio de La Plata and Kalahari cratons.

The ophiolites are tectonically intercalated with rocks of the Cambaí Complex (e.g., Cerro Mantiqueiras, Cambaizinho ophiolites) and with supracrustal rocks of the Vacacaí Group (e.g., Ibaré, Palma and Bossoroca ophiolites) (Fig. 2a). The Cambaí Complex is composed of juvenile diorite, tonalite and trondhjemite orthogneiss and by granitoids of the Lagoa da Meia Lua and Sanga do Jobim suites (Saalmann et al., 2011; Hartmann et al., 2011). The supracrustal rocks include the metavolcanosedimentary rocks of the Vacacaí Group (Remus et al., 1999) including Campestre (Gubert et al., 2016), Passo Feio (in part; (Lopes et al., 2015), Cambaizinho (Cerva-Alves et al., 2020) and Pontas do Salso (Vedana et al., 2017) formations.

These juvenile rocks are the remnants of two magmatic arcs (Saalmann et al., 2011; Hartmann et al., 2011). The older Passinho arc formed in an intra-oceanic setting and marks the first accretionary event in the Dom Feliciano Belt at ~880 Ma (Leite et al., 1998). The younger São Gabriel arc was intra-oceanic (780 – 680 Ma) and evolved to an active continental margin at ca. 700 Ma (Hartmann et al., 2011; Philipp et al., 2018; Cerva-Alves et al., 2020) and represents a second orogenic accretionary event. The São Gabriel terrane was covered by the sedimentary and volcanic sequences of the foreland Camaquã Basin (610 – 540 Ma) and was intruded by post-collisional granites (Caçapava, Jaguari, Ramada, Cerro da Cria, São Sepé Granites) associated with the third and last major tectonic event in the Sul-Riograndense Shield –the Dom Feliciano orogeny (650 – 550 Ma) (Chemale et al., 2000; Hueck et al., 2018; Philipp et al., 2018).

The eastern-central portion of the Dom Feliciano Belt – Porongos

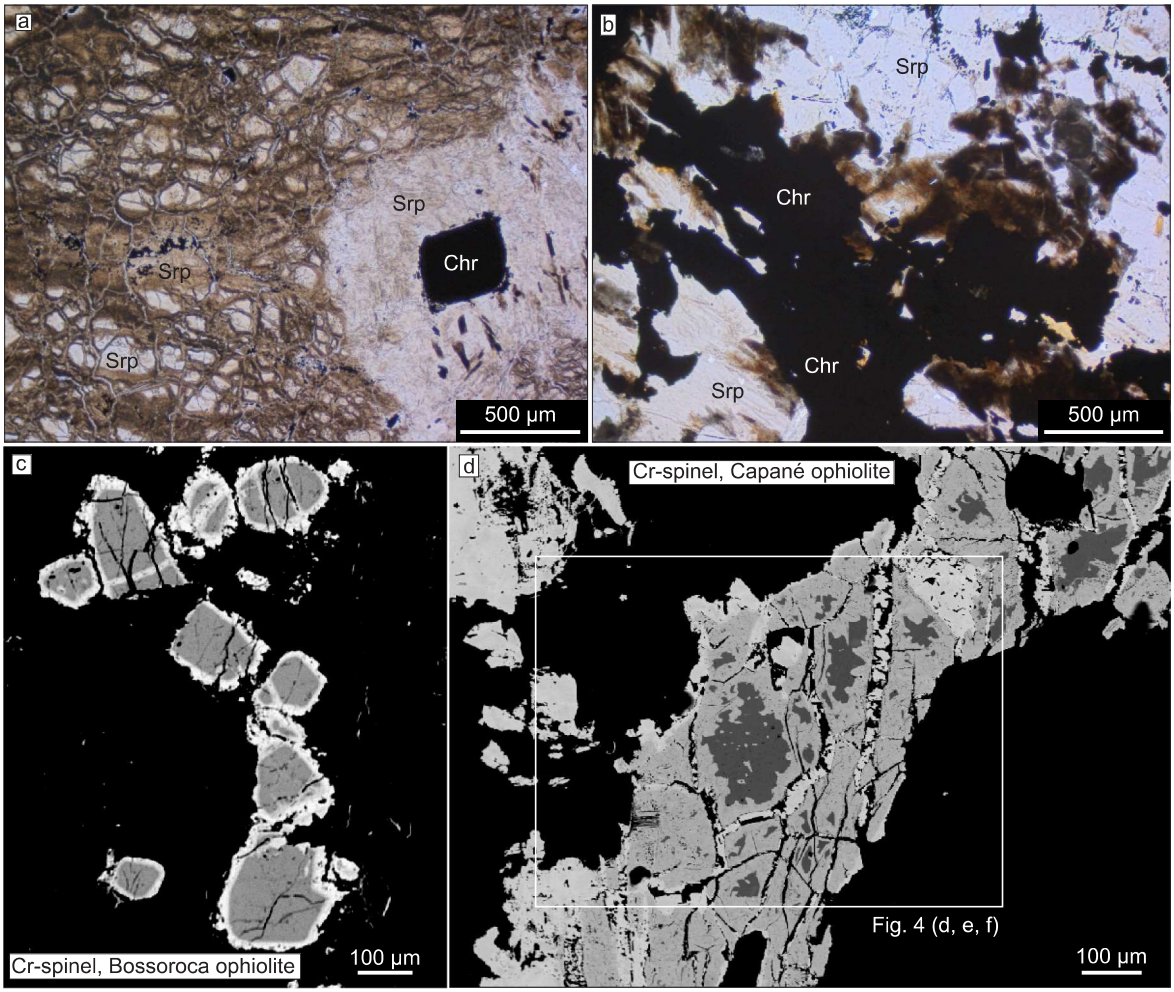

Fig. 3. (a) Thin section of serpentinite from Bossoroca ophiolite with mesh texture and disseminated Cr-spinel, plane polarized light. (b) Thin section of serpentinite from Capané ophiolite with aggregates of Cr-spinel, plane polarized light. (c) Selected backscattered electron (BSE) image of zoned Cr-spinel from Bossoroca ophiolite, displaying dark gray core and light gray rim. (d) Selected backscattered electron image of zoned Cr-spinel from Capané ophiolite.

fold-thrust belt – includes the Ediacaran Porongos Group schists, the Paleoproterozoic Encantadas Complex gneisses and Santana Formation quartzites (Hartmann et al., 2004; Pertille et al., 2015). Also known as Tijucas terrane, this belt is separated from the São Gabriel terrane in the west by the Caçapava High (Fernandes et al., 1995; Chemale et al., 2000) (Fig. 1b). Large areas, including the contact between the terranes, were covered by the sedimentary rocks of the Camaquã Basin.

The Porongos Group is the major component of the fold-thrust belt and comprises metasedimentary rocks (semipelitic schist, metapelite, quartzite) and hosts slices of ophiolites (e.g., Capané – (Marques et al., 2003; Pertille et al., 2017; Arena et al., 2018), granite, quartzite and marble (Fig. 2b). This group was part of an Ediacaran (650 – 550 Ma) foreland basin with sediments derived from the granitoids of the Pelotas Batholith and from the reworked basement (Pertille et al., 2015). The Camaquã Basin, Porongos fold-thrust belt and Pelotas Batholith formed a coeval orogenic triad (Pertille et al., 2015a, 2015b, 2017). The triad, added to the pre-1000 Ma basement and the tonian juvenile terrane, constitute the Dom Feliciano Belt.

3. Analytical methods

We integrated geological survey, petrography, electron microscopy, electron microprobe analyses (EPMA) of Cr-spinel and tourmaline, LA-ICP-MS boron isotope analyses in tourmaline and U-Pb and Lu-Hf analyses in zircon.

We selected samples of serpentinite from the Bossoroca (BM09-A, BM14-C, BM17-A) and Capané ophiolites (JP51) to make polished thin sections and mineral mounts and separated zircon from Cerro da Cria and Ramada granitic intrusions (Supplementary Table S1). Samples were prepared at 'Laboratório de Separação de Minerais, Centro de Estudos em Petrologia e Geoquímica, Instituto de Geociências, Universidade Federal do Rio Grande do Sul (CPGq-IGEO-UFRGS)', Brazil. Electron microprobe analyses (EPMA) were undertaken at Universidade Federal de Ouro Preto, Laboratory of Microscopy and Microanalysis (DEGEO-UFOP-Brazil) using a JEOL JXA-8230 superprobe, equipped with five wavelength dispersive spectrometers (WDS). Analytical procedures followed methodology established at UFOP (e.g., Hartmann et al., 2019). Operating conditions were 15 kV accelerating voltage, 20nA beam current and 5 µm beam diameter. Boron isotopes by LA-ICP-MS U-Pb and Lu-Hf isotopes were determined at Departamento de Geologia of Universidade Federal de Ouro Preto, Minas Gerais, Brazil, with a Thermo-Scientific Neptune Plus multi-collector ICP-MS. The procedures follow the pattern described in Cerva-Alves et al. (2020), Hartmann et al. (2019) and Schannor et al. (2019). Mineral abbreviations follow Whitney and Evans (2010). Methodology is given in Supplementary Text S1.

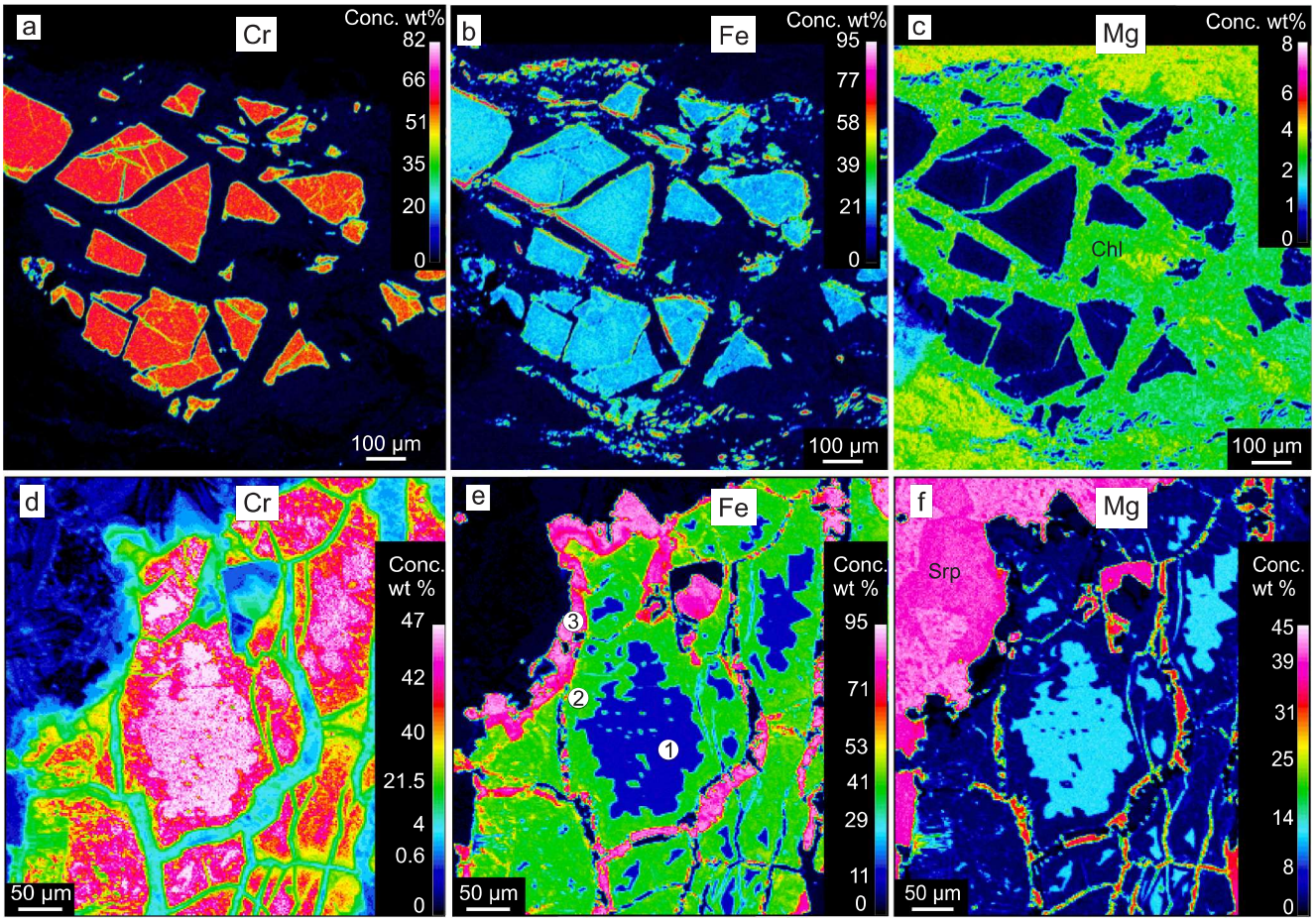

Fig. 4. Quantitative characteristic X-ray maps of Cr-spinel. (a-c) Bossoroca ophiolite, showing two zones. (d-f) Capané ophiolite, showing three zones (Cr-spinel 1, 2 and 3) similar to BSE images.

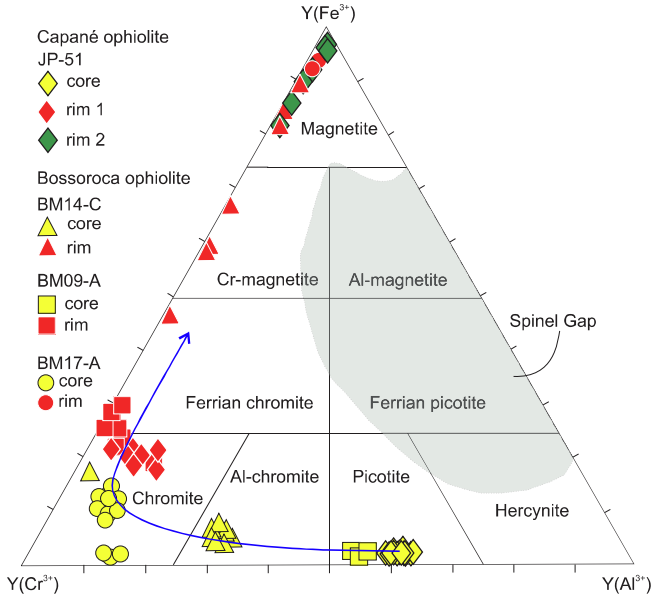

Fig. 5. Triangular classification diagram of Cr-spinel, Bossoroca and Capané ophiolites. $Y(Cr^{3+}) = Cr/(Cr + Fe^{3+}+Al)$; $Y(Fe^{3+}) = Fe^{3+}/(Cr + Fe^{3+}+Al)$; $Y(Al^{3+}) = Al/(Cr + Fe^{3+}+Al)$ (modified from Gargiulo et al., 2013); (spinel gap after Barnes and Roeder, 2001).

4. Results

4.1. Field relationships

The Bossoroca ophiolite consists of several serpentinite bodies, volcanoclastic rocks, and chloritite in the studied southern portion. Serpentinite hosts Cr-spinel and the associated chloritite contains tourmaline.

Serpentinites form hilly outcrops in grasslands approximately 1 km long and 200 m wide dipping ~60° to NNW. Serpentinite is green to dark grey, fine to medium grained and shows mesh texture with veins of opaque minerals; Cr-spinel is accessory. In some intensely altered portions, serpentinite is light grey. The two post-tectonic intrusions – Cerro da Cria and Ramada Granites, are in direct, covered contact with the ophiolite.

Chloritites (chl > 90 vol%) form 0.5–1.0 m-long loose blocks enclosed in serpentinite. Most blocks are massive but some have incipient foliation. Chlorite is dark green and shows lepidoblastic texture. Tourmaline is dispersed in chloritite and is better identified in sawed, polished hand samples.

Sample JP51 is a chromitite enclosed in serpentinite from the Capané ophiolite. These rocks are hosted in schists from the Porongos Group and covered by rocks of the Camaquã Basin and Rio Bonito Formation, Paraná Basin.

4.2. Petrography and mineral chemistry

Three samples of serpentinite, one sample of chloritite from the Bossoroca ophiolite and one sample (JP51) of serpentinite from the

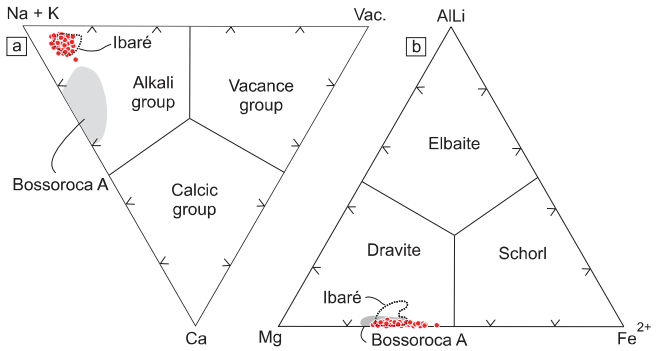

Fig. 6. Triangular classification diagrams of tourmaline (modified from Arena et al., 2020). (a) Classification according to the occupation of X site of tourmaline. (b) Classification according to the occupation of Y site of tourmaline. Ibaré compositions from Arena et al. (2020) and Bossoroca A from Hartmann et al. (2019).

Capané ophiolite were selected for petrography and mineral chemistry (results in Supplementary Tables S2–S6). In thin section, serpentinite from the Bossoroca ophiolite has mesh texture and is composed of serpentine, tremolite, magnetite, chlorite and Cr-spinel. Chloritite has lepidoblastic texture; some crystals form radial bundles. This metasomatic rock is composed of chlorite and accessory apatite, magnetite and monazite. WDS analyses were carried out on Cr-spinel from serpentinite and tourmaline from chloritite.

4.2.1. Cr-spinel in serpentinite

Modal composition of serpentinite from the Bossoroca ophiolite is serpentine (75–90 vol%), tremolite (10 vol%), magnetite (7–10 vol%), forsterite (5 vol%), chlorite (4 vol%) and Cr-spinel (3 vol%) (Fig. 3a). Serpentine has mesh texture, is fine to medium grained and also fills fractures. Tremolite presents radial growth with crystals up to 0.7 mm in size. Magnetite fills veins and fractures in serpentine, also occurring in rims of Cr-spinel that were formed during metamorphism. Chlorite is usually associated with Cr-spinel showing reaction textures. Accessory Cr-spinel in serpentinite is subhedral and up to 500 μm in size (Fig. 3a). Cr-spinel shows distinct core and rim zoning in BSE (Fig. 3c). Cores are homogeneous and dark grey and surrounded by thin, light gray rims. Some Cr-spinel crystals are broken with chlorite growth between pairs of fragments.

EPMA analyses and characteristic X-ray maps of Cr-spinel from Bossoroca ophiolite show cores with high Al_2O_3, Cr_2O_3 and low TiO_2 and MgO concentrations (Fig. 4a, b, c; Supplementary Tables S2–S4). Rims are enriched in Fe_2O_3. This indicates a trend of alteration of Cr-spinel from aluminous cores (picotite, Al-chromite and chromite) to ferric rims (Fe-chromite, Cr-magnetite and magnetite) (Fig. 5). FeO is homogeneous. Chromium numbers – Cr# = Cr/(Cr + Al), vary in cores from 0.57 to 0.74 and Mg# = Mg/(Mg + Fe^{2+}) vary from 0.14 to 0.26; Cr# of the rims vary from 0.87 to 0.97 and Mg# from 0.01 to 0.19. Chemical zoning of chromite is reflected in the mineral classification diagram (Fig. 5).

Serpentinite of Capané ophiolite has a mineral assemblage of serpentine (85 vol%), Cr-spinel (10 vol%) and magnetite (5 vol%) (Fig. 3b). Pseudomorphic texture and magnetite veins are common in serpentinites. Cr-spinel shows three zones in BSE images (Fig. 3d): homogeneous dark core (spinel 1), medium-gray mantle (spinel 2) and light gray rim (spinel 3). EPMA analyses and characteristic X-ray maps of Cr-spinel from the Capané ophiolite (Fig. 4d, e, f) show homogeneous cores with high Al_2O_3 (26.62–28.19 wt%), Cr_2O_3 (47.74–45.64 wt%) and MgO (14.42–15.53 wt%) (Supplementary Table S5). Spinel classification diagram indicates picotite in the cores (Fig. 5). Cr# varies from 0.51 to 0.53 and Mg# from 0.66 to 0.69. Mantle of spinel 2 has lighter gray tone in BSE images. EPMA analyses and characteristic X-ray maps show low Al_2O_3 (1.56–4.46 wt%), Cr_2O_3 (36.82–39.92 wt%), MgO

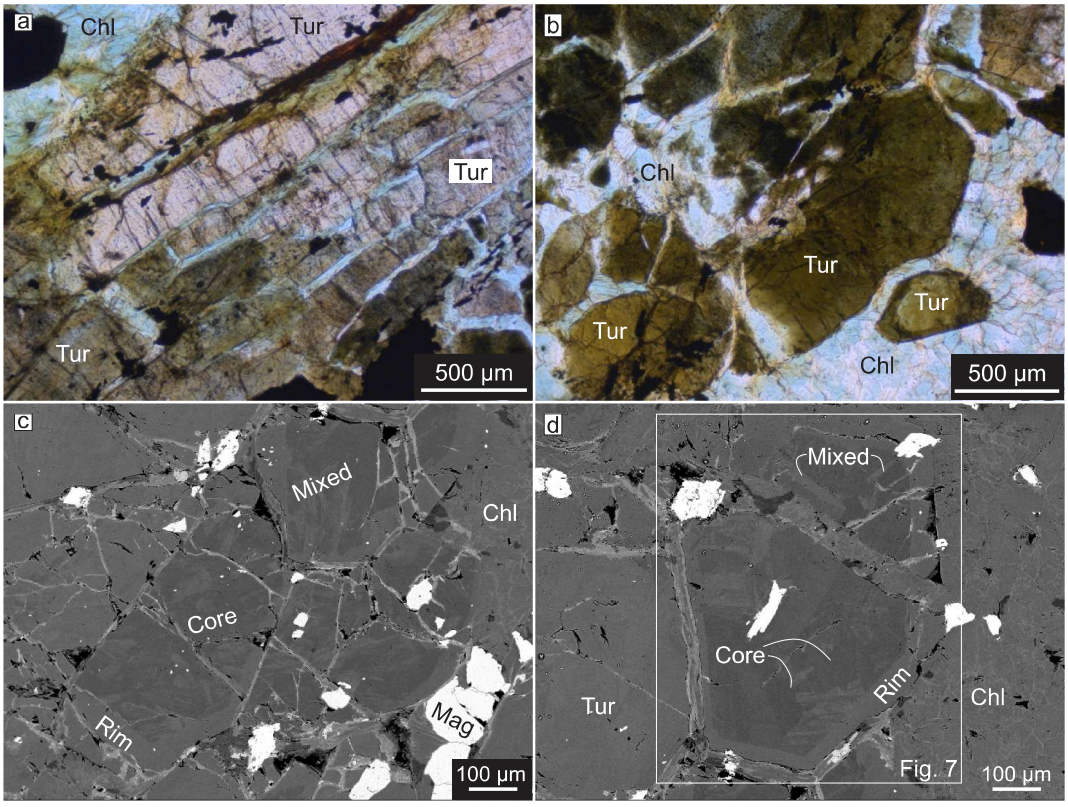

Fig. 7. (a-b) Photomicrographs of chloritite with dravite, Bossoroca ophiolite, plane polarized light. (c-d) Selected backscattered electron images of zoned tourmaline.

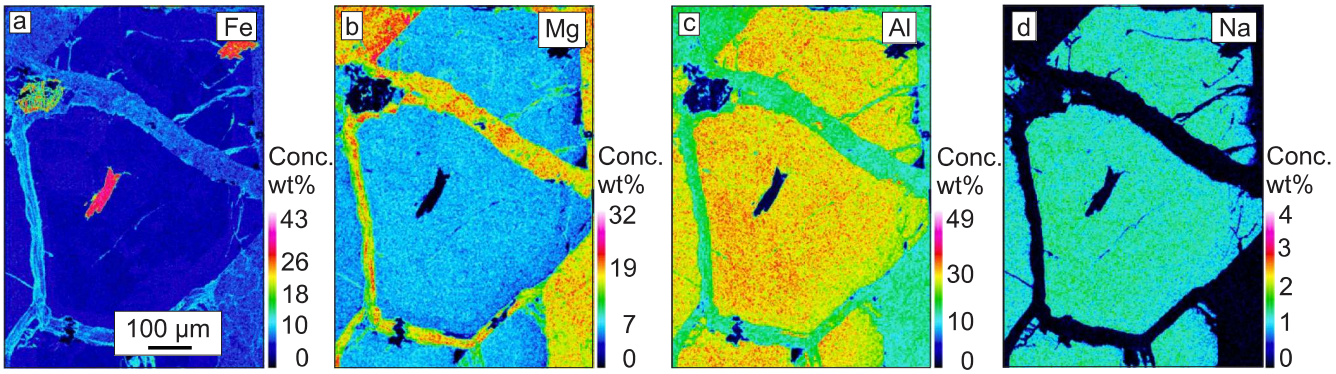

Fig. 8. (a-d) Quantitative characteristic X-ray maps of dravite, Bossoroca ophiolite. Core, rim and mixed zone are visible in the compositional map of Fe.

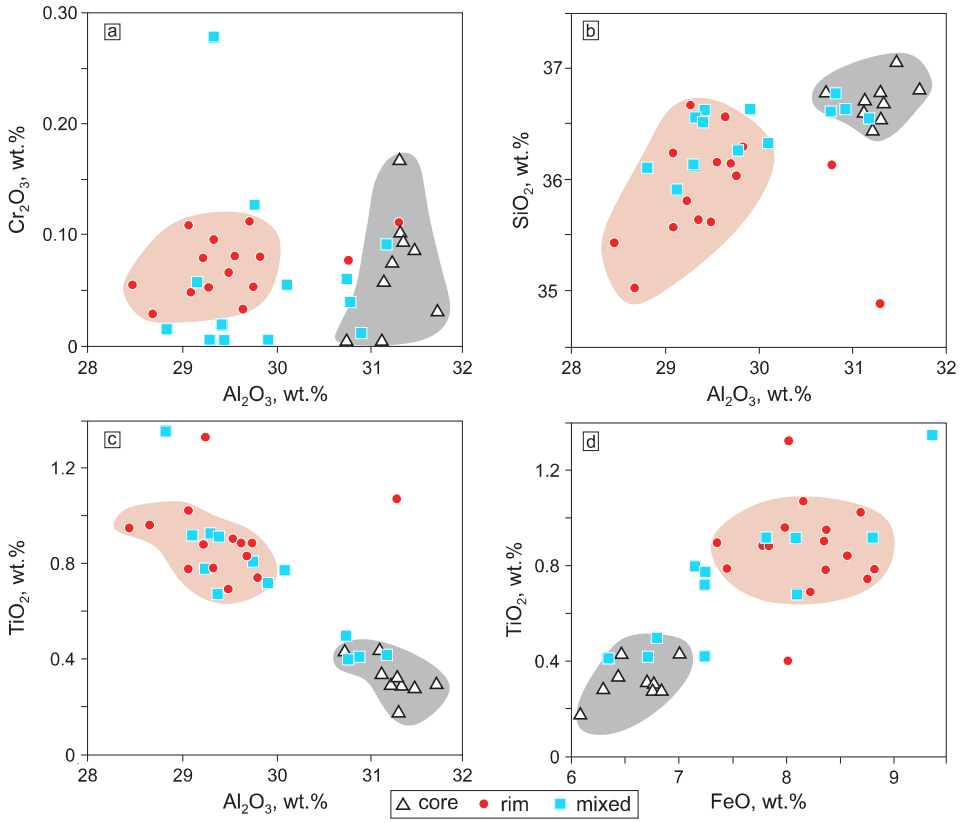

Fig. 9. Binary diagrams displaying compositional variation between cores, rims and mixed zones of tourmaline.

(2.96–5.50 wt%) and high Fe_2O_3 (22.24–27.56 wt%). In the spinel classification diagram, these mantles are chromite. Values of Cr# are high and vary from 0.85 to 0.94; Mg# are low from 0.19 to 0.35. BSE images, EPMA analyses and characteristic X-ray maps of spinel 3 show a light gray portion in contact with spinel 2. Spinel 3 is magnetite (Fig. 5).

4.2.2. Dravite in chloritite

Chloritite samples consist of Mg-chlorite (>85 vol%), apatite (7 vol %), magnetite (5 vol%) and accessory monazite. One sample of chloritite (BM16-T) has tourmaline in the mineral assemblage. Low U concentrations in monazite from the chloritite precluded in situ U-Pb age determination.

EPMA results (n = 37) classify tourmalines as dravite from the alkali group (Fig. 6; Supplementary Table S6). This classification is similar to dravites designated Bossoroca A (Hartmann et al., 2019) and Ibaré (Arena et al., 2020) described in the juvenile terrane. Dravite is contained in chlorite and shows light pink to dark green pleochroism and internal zoning (Fig. 7a, b). Crystals are euhedral with sizes up to 0.8 cm. Cataclasis fractured and broke crystals, fractures filled with chlorite. Integrated observation of BSE images, characteristic X-ray maps and EPMA analyses of dravite displays three zones with compositional differences (core, rim and mixed zone) (Fig. 7c, d; Fig. 8; Fig. 9a, b, c, d; Supplementary Fig. S1). The cores are heterogeneous with darker gray portions, the mixed zones have lighter portions. Rims are homogeneous, light gray and surround the cores along straight, crystallographic faces (Fig. 7c, d). Characteristic X-ray map of Fe shows core, mixed zone and rim (Fig. 8a), whereas Mg, Al and Na outline the rim (Fig. 8b, c and d). Heterogeneous cores have high SiO_2 (36.12–37.05 wt%) and Al_2O_3 (28.32–31.7 wt%) concentrations, low TiO_2 (0.18–1.36 wt%) and FeO (6.08– 9.38 wt%). Rims have high FeO (7.36–8.82 wt%), TiO_2 (0.69–1.33 wt%) and low SiO_2 (34.88–36.66 wt%) and Al_2O_3 (28.45–31.29 wt%) compared to the cores (Fig. 9). Compositions of mixed zones are gradational between cores and rims and have high FeO and TiO_2 (Fig. 9).

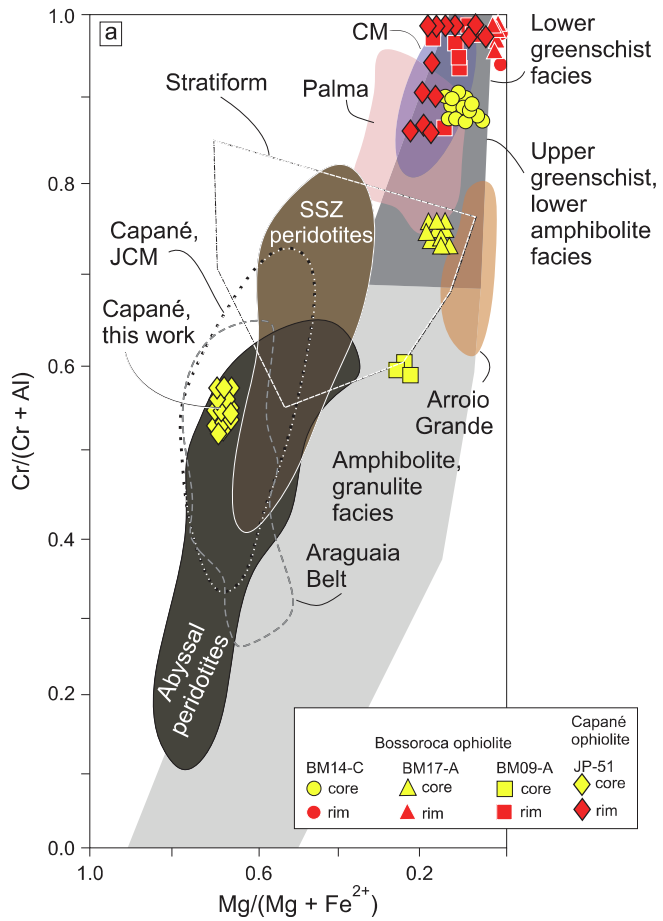

Fig. 10. Mg# x Cr# petrogenetic classification diagram of Cr-spinel, Bossoroca and Capané ophiolites (modified from Hartmann and Chemale, 2003). Ophiolite and stratiform fields Irvine (1967) and Barnes and Roeder (2001). Metamorphic fields from Evans and Frost (1975), Suita and Strieder (1996). Abyssal peridotites field from Dick and Bullen (1984) and SSZ peridotites field from Parkinson and Pearce (1998). Cr-spinel from other ultramafic rocks, Brasiliano Orogen also displayed; CM = Cerro Mantiqueiras (Hartmann and Chemale, 2003); Palma = Palma ophiolite (Hartmann et al., 2000); Arroio Grande = Arroio Grande ophiolite (Ramos et al., 2017); Capané, JCM = Capané ophiolite (Marques, 1996); Araguaia Belt (ophiolites from Kotschoubey et al., 2005; Hodel et al., 2019).

4.3. Boron isotopes of dravite

In situ B isotopes analyses of distinct tourmaline zones (cores, mixed zones and rims) yeld significant isotopic variation (Supplementary Table S7). Cores have $\delta^{11}B$ values of + 1.95 to + 2.50‰ (peak at + 2.30) (n = 7), mixed zones (n = 11) have $\delta^{11}B$ values of + 0.26 to + 1.99‰ (peak at + 1.16) and rims (n = 28) have $\delta^{11}B$ values of −0.56 to + 2.42‰ (peak at + 1.42).

4.4. Zircon U-Pb-Hf isotopes

U-Pb-Hf isotope data are listed in Supplementary Tables S8 and S9. Zircon crystals from the two granites are mostly euhedral, homogeneous, little fractured, and show aspect ratios 2:1 (Supplementary Fig. S2). Thirty zircons from the Ramada Granite yield concordia age (Fig. 12a) of 578 ± 3.2 Ma with MSWD of concordance = 0.066. Th/U ratios of zircon are 1.47–5.69, considered magmatic (Hartmann et al., 2000). Zircons from the Cerro da Cria Granite yield an intercept U-Pb age (Fig. 12b) of 612 ± 12 Ma with MSWD of concordance = 0.087. Some analyses show discordant ages younger than 570 Ma. These younger ages are interpreted as due to Pb loss. Th/U ratios vary between 1.49 and 2.84.

The εHf values for Cerro da Cria Granite vary from −8 to −13 and for Ramada Granite from −16 to −25. Negative, subchondritic εHf values indicate contribution from old continental crust during melting of the granites (Fig. 13).

5. Discussion

5.1. Evolution of Bossoroca ophiolite

Cr-spinel is a petrogenetic indicator in mafic and ultramafic rocks. However, Cr-spinel is susceptible to modifications during alteration and subsequent prograde metamorphism of host rocks, thus affecting the petrogenetic interpretation and erasing the magmatic history (Kimball, 1990; Barnes, 2000). The serpentinites of the Bossoroca ophiolite have accessory, zoned Cr-spinel. Despite preserved magmatic core and rim textures visible in BSE images, mineral chemistry indicates modification of composition during metamorphism. Low Mg# for cores (0.26–0.14) and rims (0.19 – 0.01) and increase in Cr# (0.57–0.97) from cores to rims in Cr-spinel of serpentinite from the Bossoroca ophiolite demonstrate alteration during metamorphism under greenschist and low amphibolite facies (Fig. 10) (Kimball, 1990; Suita and Strieder, 1996). The low values of Mg# reflect exchange of Mg^{2+} and Fe^{2+} between Cr-spinel and other silicates during metamorphic alteration of the ultramafic rocks (Barnes, 2000; González-Jiménez et al., 2009; Bhat et al., 2019). The mineral assemblage tremolite + talc + forsterite + chlorite in serpentinite from the Bossoroca ophiolite indicates low amphibolite facies metamorphism (Barnes and Roeder, 2001). These results are compatible with the low amphibolite facies conditions described by Hartmann et al. (2019) in the northern portion of the Bossoroca ophiolite.

Tourmaline in ophiolite is a powerful tool in the study of the evolution of oceanic rocks during interaction with seawater. The mineral is refractory, capable of accommodating many elements and is stable during most geological processes. Tourmaline is widely used in geochemical and boron isotope studies of continental and oceanic crust environments, because the mineral maintains the isotopic composition after crystallization (Henry and Dutrow, 1996; Trumbull et al., 2013; Grew et al., 2015; Farber et al., 2015; Trumbull and Slack, 2018; Hartmann et al., 2019; Arena et al., 2020).

Boron isotopic ratios show large variations in natural systems. The main geochemical reservoirs of B are the continental crust (average $\delta^{11}B$ = -10‰), mantle (average $\delta^{11}B$ = -7‰) and seawater (average $\delta^{11}B$ = +39.6‰) (Fig. 11) (Van Hinsberg et al., 2011; Yamaoka et al., 2015; Marschall and Foster, 2018). Fresh mantle (MORB, OIB) has very low B concentrations (0.060 ppm) and relatively uniform $\delta^{11}B$ = −7‰. Serpentinites have high B concentrations (10–91 ppm) and high $\delta^{11}B$ values (+7 to +19.9‰) compared to fresh mantle. The increase in B concentrations and the high $\delta^{11}B$ values in serpentinites are due to the interaction of seawater with the mantle rocks (Marschall et al., 2006, 2018).

Previous studies of the Bossoroca ophiolite described in the northern portion a massive tourmalinite close to serpentinite and amphibolite (massive tourmalinite – Bossoroca A; (Hartmann et al., 2019; Werle et al., 2019). Bossoroca A tourmaline is dravite with three distinct zones: Tur 1, 2 and 3. Tur 1 is homogeneous and has $\delta^{11}B$ = 1.8‰, Tur 2 is heterogeneous with $\delta^{11}B$ = −1 to +0.4‰. Irregular contacts between the two zones led to the interpretation that Tur 2 formed by alteration and replacement of Tur 1. Tur 3 has $\delta^{11}B$ = −8.2 to −9.2 and was interpreted as formed from metamorphic fluids in the greenschist facies after obduction (Hartmann et al., 2019). Massive tourmalinite from the Ibaré ophiolite has homogeneous dravite with $\delta^{11}B$ = +3.2 to +5.2‰ that formed in altered oceanic crust (Arena et al., 2020).

We identified a second occurrence of tourmaline in the Bossoroca ophiolite (Tourmaline B). This dravite occurs included in magnesian chlorite from chloritite enveloped by serpentinite. The three zones identified in BSE images (cores, rims and mixed zones) show

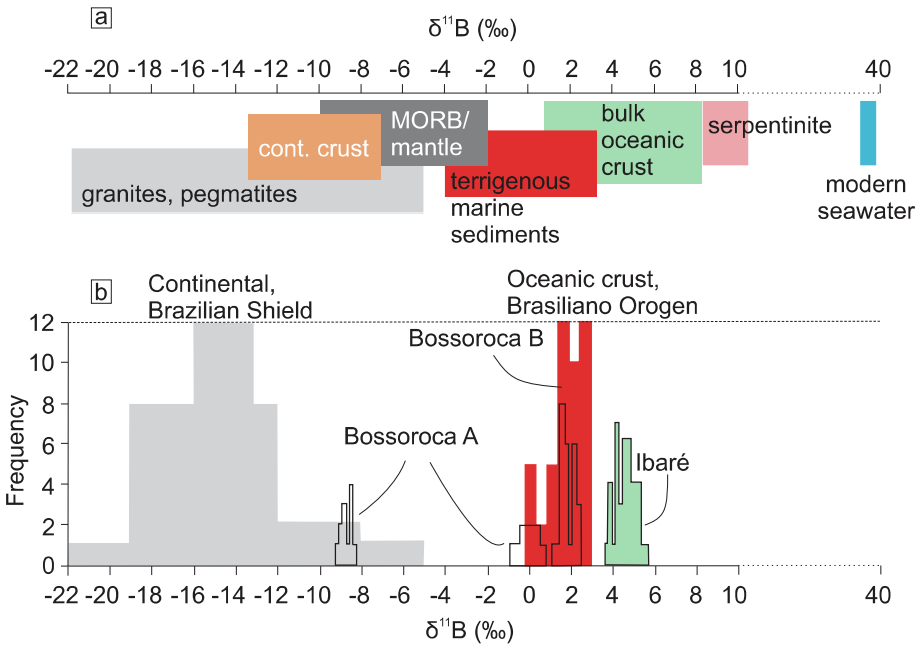

Fig. 11. Histogram of boron isotopic compositions of tourmaline from Bossoroca and Ibaré ophiolites. (a) Different sources of boron from main geological environments. Data from Farber et al. (2015) and Marschall and Foster (2018). (b) $\delta^{11}B$ values of dravite from the southern Bossoroca ophiolite (Bossoroca B – filled red). Continental Brazilian Shield field from Garda et al. (2009), Trumbull et al. (2013), Albert et al. (2018). Oceanic crust fields of Ibaré (Arena et al., 2020) and Bossoroca A (black outline) from Hartmann et al. (2019). (For interpretation of the references to colour in this figure legend, the reader is referred to the web version of this article.)

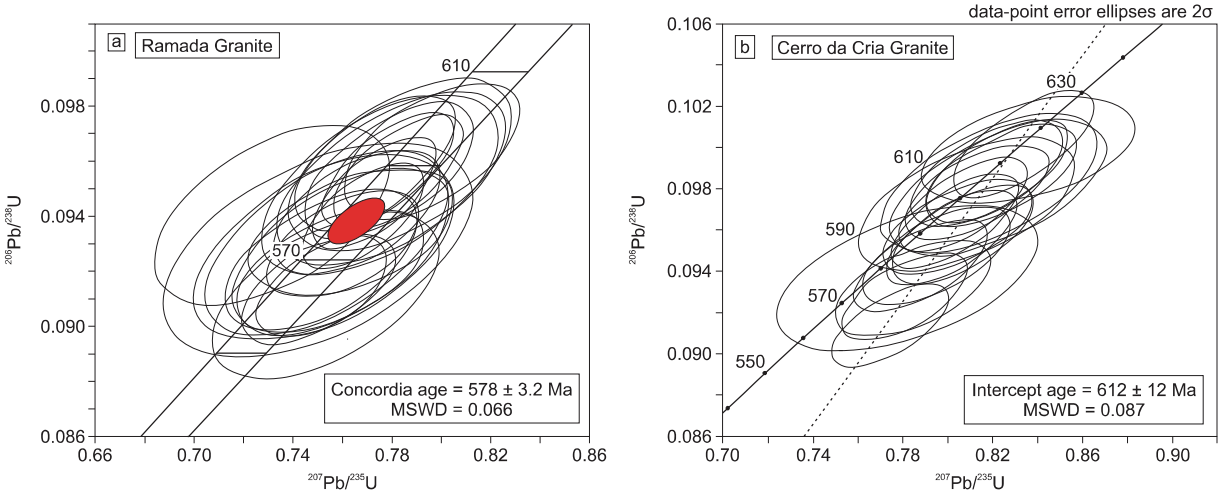

Fig. 12. U-Pb concordia diagrams for igneous zircon from (a) Ramada Granite and (b) Cerro da Cria Granite.

correspondence between mineral chemistry and boron isotopic composition. The different zones (cores, rims and mixed zones) identified in BSE images of dravite and in the characteristic X-ray maps indicate the occurrence of two events of tourmaline growth, which is supported by mineral chemistry and boron isotopes. The first event is recorded in cores that have high $\delta^{11}B$ values (+1.95 to + 2.50‰), low Fe^{2+} (0.826 – 0.993 apfu), Ti (0.02 – 0.09 apfu) and high Al (5.78 – 6 apfu) and Si (5.96 – 6.01 apfu) compared to the rims. The higher $\delta^{11}B$ and large chemical difference between core and rim seen in the binary diagrams suggest formation of tourmaline cores by direct interaction with hydrothermal seawater with high fluid/rock ratio. Rims grew outwards from the cores and have low $\delta^{11}B$ values (−0.56 to +2.42‰), high Fe^{2+} (1.01 – 1.24 apfu), Ti (0.05 – 0.16 apfu) and low Al (5.65 – 5.94 apfu) and Si (5.75 – 6.0 apfu) compared to the cores. Rims record the second episode of tourmaline formation within the oceanic crust with influence of terrigenous sediments. Dravite (Tourmaline B) formed below the interface of seawater with oceanic crust with composition controlled by host rock and hydrothermal fluids. Positive $\delta^{11}B$ values of Tourmaline B point to the formation of dravite in altered oceanic crust from seawater-derived hydrothermal fluids present in terrigenous marine sediments (Fig. 11). The decrease in $\delta^{11}B$ values between tourmaline cores and rims is explained by reaction with seawater that had small fluid/rock ratios (e.g., Yamaoka et al., 2015). Mixed zones portions have $\delta^{11}B$ and chemistry that vary between the compositions of cores and rims. The mixed zones correspond to portions of cores partly altered during formation of rims (second event of tourmaline growth). Cores with high $\delta^{11}B = +2.30‰$ and low Fe^{2+} (0.83 to 0.99 apfu) are similar and comparable to Tur 1 described in Tourmaline A by Hartmann et al. (2019). Tur 1 is homogeneous and has high $\delta^{11}B = +1.8‰$ and low Fe^{2+} (0.74 – 0.85 apfu). Rims in Bossoroca Tourmaline B are comparable with Tur 2 of Hartmann et al. (2019), reflected by heterogeneous structure in BSE and characteristic X-ray maps with lower $\delta^{11}B = -1$ to +0.4‰ and higher Fe^{2+} (0.85 – 1.25 apfu). Tourmaline type Tur 3 described in Bossoroca A was not identified in Tourmaline B.

The difficulty of dating ultramafic rocks and characterizing oceanic pre-obduction processes was overcome by the systematic study of metasomatic rocks in the ophiolite. Metasomatic rocks in ophiolites include commonly chloritite, tourmalinite, rodingite, and albitite, which

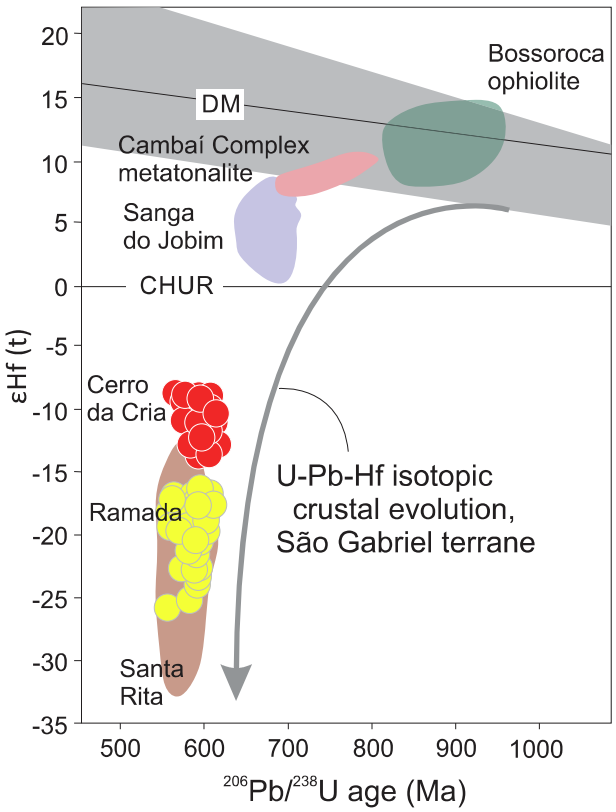

Fig. 13. εHf values versus U-Pb ages of zircon from Ramada and Cerro da Cria Granites. Santa Rita Granite from Arena et al. (2017). SJG = Sanga do Jobim Granite and CC = Cambaí Complex from Cerva-Alves et al. (2020). Bossoroca ophiolite field from Hartmann et al. (2019). DM = depleted mantle, CHUR = chondritic uniform reservoir. Highlighted field is depleted mantle evolution from Gerdes and Zeh (2006).

concentrate Zr during their formation and thus favors zircon crystallization (Arena et al., 2016, 2017, 2018; Hartmann et al., 2019; Cerva-Alves et al., 2020). Zircon included in tourmaline from tourmalinite in the Bossoroca ophiolite (Tourmaline A) was dated and characterized as oceanic in composition. The U-Pb age is 920. 4 ± 9.8 Ma, with oceanic signature (U/Yb < 0.1) and origin from depleted mantle with εHf = +12 (Hartmann et al., 2019) marking the earliest mantle-derived composition in the São Gabriel terrane.

A continuum of U-Pb-Hf isotopic evolution of the crust is observed in the terrane from mantle-derived compositions in the Bossoroca ophiolite (e.g., Hartmann et al., 2019) evolving to Cambaí Complex metatonalite and Sanga do Jobim Granite (Cerva-Alves et al., 2020) (Fig. 13). The descending curve indicates interaction with continental crust in the formation of the Sanga do Jobim Granite. A strong descent in εHf occurred during formation of Cerro da Cria and Ramada Granites. Zircon from the Cerro da Cria granite has age = 612 ± 12 Ma, εHf = −8 to −13; Ramada granite is 578 ± 3.2 Ma, εHf = −16 to −25, altogether indicating melting of old continental crust in the underburden of the terrane. This interpretation by Remus et al. (1999) based on isotopic geochemistry was corroborated by magnetotelluric investigations of Bologna et al. (2019) that show presence of craton underneath the juvenile São Gabriel terrane.

The evolution of the Bossoroca ophiolite started in the mid-ocean ridge with the fragmentation of Rodinia supercontinent at 920 Ma (Hartmann et al., 2019). The pre-obduction processes consist of intense serpentinization and metasomatism of the Tonian oceanic crust and mantle. A long-lived history of heated seawater infiltration altering the rocks formed serpentinites, metasomatic chloritite and zoned dravite. Dravite from the southern Bossoroca ophiolite formed below the interface of seawater with oceanic crust and has compositions controlled by host rock and hydrothermal fluids. Dark (in BSE) tourmaline cores formed directly in contact with seawater. Rims formed with less influence of the seawater and the mixed zone represents alteration of cores by fluids. This process can be compared to modern mid-Atlantic ridge in the Lost City hydrothermal system described by Boschi et al. (2008). In the system, seafloor hydrothermal activity formed serpentinites with high boron concentration (34 – 91 ppm) and high $\delta^{11}B$ values (+11 to +16‰) and metasomatic rocks (chlorite-rich talc schist). The data indicate extensive serpentinization dominated by seawater at temperatures between 150 and 250 °C with high fluid/rock ratio (Boschi et al., 2008).

The low amphibolite facies metamorphic event altered the Cr-spinel composition during obduction of the ophiolite over the São Gabriel arc. Overthrusting of the juvenile São Gabriel terrane and ophiolites over the Rio de La Plata Craton occurred between 660 Ma (Cerva-Alves et al., 2020) and 612 Ma (this work) and triggered a descending curve of εHf from mantellic to continental crust.

5.2. *Evolution of Capané ophiolite*

Podiform chromitites in ophiolites support the understanding of geological setting of ultramafic rocks (e.g., Rollinson, 2008; Miura et al., 2012; Dechamps et al., 2013; González-Jiménez et al., 2014; Mohanty et al., 2018; Hodel et al., 2019). Cr# of Cr-spinel allows the distinction between peridotites (and related serpentinites) formed in abyssal environments and in suprasubduction zones (Dick and Bullen, 1984; Dechamps et al., 2013). Cr-spinel of abyssal peridotites has low Cr# (0.20 < Cr# < 0.60), whereas in subduction-related rocks (SSZ peridotites) the Cr-spinel has higher Cr# (>0.60) (Dick and Bullen, 1984; Rizeli et al., 2016). Cr-spinel in ophiolite records the nature of ancient upper mantle, young oceanic mantle and processes of melt formation (González-Jiménez et al., 2014).

The Capané ophiolite is composed of lenses of serpentinite, magnesian schist, talc schist, podiform chromitite and rodingite (Jost and Hartmann, 1979; Marques et al., 2003; Arena et al., 2018). The recognition of primary compositions of Cr-spinel establishes these rocks as a fragment of the oceanic lithosphere in the accretionary Brasiliano Orogen. The cores of Cr-spinel from the Capané ophiolite (spinel 1 – picotite) record high Mg# (0.69–0.66) and low Cr# (0.53–0.51) consistent with formation in abyssal peridotites (Fig. 10). Abyssal peridotites form in the mid-ocean ridge environment and are residues of adiabatic decompression melting mostly in slow to ultraslow spreading ridges (Dechamps et al., 2013; Warren, 2016). The rims (spinel 2 – chromite, spinel 3 – magnetite) decrease in Cr and Mg contents and increase in Fe compared to the core. Lower Mg# and higher Cr# in rims indicate that chromite and magnetite rims formed by alteration during low-grade metamorphism (Fig. 10) (Ismalil, 2009; González-Jiménez et al., 2009; Azer, 2014).

Podiform chromitites from the Araguaia Belt include Cr-spinel with primary mantle-derived composition, as pioneering description in Brasiliano Orogen ophiolites (Kotschoubey et al., 2005; Hodel et al., 2019). In the Dom Feliciano Belt, mantle-derived composition of Cr-spinel from the Capané ophiolite was recognized by Marques (1996) and is described in this work. In contrast to the metamorphic composition of Cr-spinel from other ophiolites in the Dom Feliciano Belt, fresh cores of the Capané spinel have high Al_2O_3 (26.62–28.19 wt%), Cr_2O_3 (47.74–45.64 wt%) and MgO (14.42–15.53 wt%) and very low TiO_2 (<0.06 wt%). These compositions are characteristic of primary, mantle-derived Cr-spinel described for podiform chromitites from other ophiolites (e.g., Zhou et al., 2001; Azer, 2014; González-Jiménez et al., 2014).

The Capané ophiolite marks the closure of the Adamastor ocean in the evolution of West Gondwana (Arena et al., 2018). The evolution of the ophiolite started in the mid-ocean ridge environment in a slow to ultraslow spreading ridge. Abyssal peridotites are considered the protoliths of the serpentinites consistent with the primary composition of

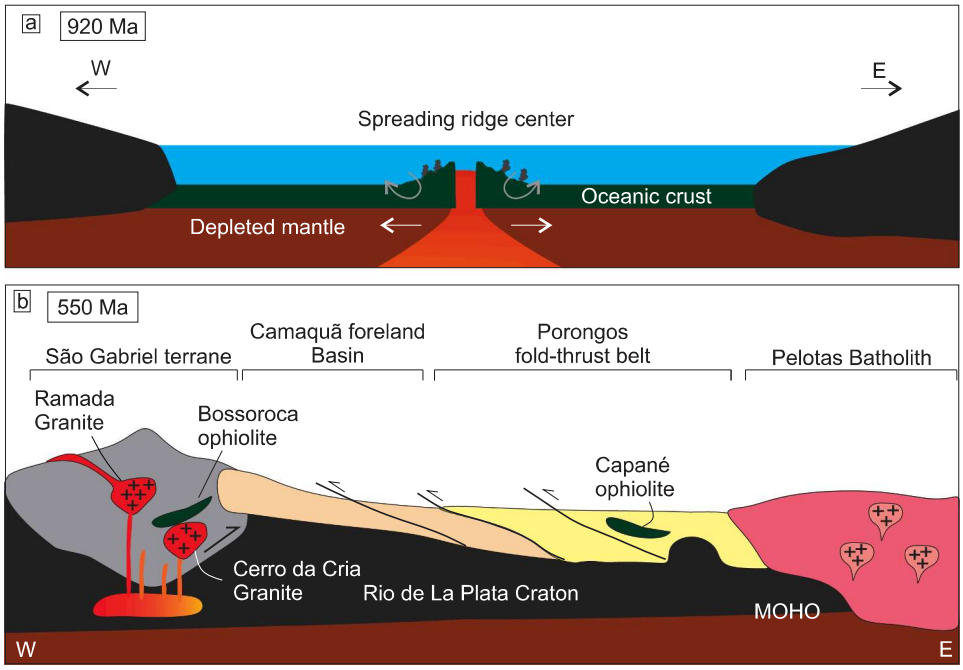

Fig. 14. (a) Metasomatic and serpentinization events in the formation of Neoproterozoic oceanic crust at 920 Ma. (b) Final geotectonic scenario of the Sul-Riograndense Shield at 550 Ma with the emplacement of Ramada and Cerro da Cria granites into São Gabriel terrane (modified from Saalmann et al., 2011; Hartmann et al., 2019; Pertille et al., 2017 and Arena et al., 2018).

Cr-spinel cores. Intense metasomatism produced rodingites. Previous studies of metasomatic zircon from a rodingite blackwall in the Capané ophiolite yielded ages of 793 ± 0.9, 757 ± 2.1, 715 ± 2.2 Ma (Arena et al., 2018). These ages were interpreted as multiple alteration events in the mantle. Values of εHf = +10.7 to + 15 and trace elements of zircon (e.g., U/Yb < 0.1) indicate that the metasomatic rock was formed in an oceanic crust environment (Arena et al., 2018). The obduction occurred during the collision that formed the Porongos fold-thrust belt at 650–570 Ma (Arena et al., 2018).

Finding and analyzing some rare and informative minerals in the Bossoroca and Capané ophiolites integrated with U-Pb dating and Lu-Hf isotopes in zircon from the Ramada and Cerro da Cria Granites fostered the understanding of the evolution of the mantle, oceanic and continental crust in the southern Brasiliano Orogen. The evolution of Neoproterozoic oceanic crust in southern Brasiliano Orogen started at 920 Ma with metasomatic events forming chloritites with tourmaline with positive $\delta^{11}B$ values, indicating altered oceanic crust from seawater-derived hydrothermal fluids present in terrigenous marine sediments. Intense serpentinization altered abyssal peridotites from spreading ridge center environment (Fig. 14a). Subduction zones are the fundamental driver for the incorporation of oceanic crust and mantle into continental margins or island arcs (Dilek and Furnes, 2014). The process of closure of Adamastor ocean resulted in preservation of oceanic crust and mantle in different geotectonic settings in southern Brasiliano Orogen. The final geotectonic scenario at 550 Ma was marked by granitic intrusions triggered by melting of old continental crust beneath São Gabriel juvenile terrane (Fig. 14b). Characterizing the pre-obduction processes that occurred in ophiolites is key to the reconstruction of the geodynamic evolution of the accretionary, oceanic stage of the Brasiliano Orogen in the consolidation of Gondwana Supercontinent.

6. Conclusions

Tonian-cryogenian evolution of ophiolites in the southern Brasiliano Orogen started at 920 Ma with crystallization of zircon and dravite in an oceanic ridge of the proto-Adamastor Ocean during intense serpentinization of abyssal peridotite consistent with mantle-derived Cr-spinel cores. Oceanic crust was preserved in the southern Bossoroca ophiolite as evidenced by heavy B isotopic compositions of tourmaline. Overthrusting of assembled oceanic crust and São Gabriel arc onto the Rio de La Plata Craton resulted in melting of cratonic rocks and intrusion of Ediacaran granites consistent with negative zircon εHf values. The agglomeration of Gondwana involved overthrusting of oceanic crust + mantle sections + intra-oceanic arcs over the Paleoproterozoic basement.

CRediT authorship contribution statement

M. Werle: Writing - review & editing, Writing - original draft, Formal analysis, Conceptualization, Data curation, Investigation, Methodology, Validation, Visualization. **L.A. Hartmann:** Writing - review & editing, Writing - original draft, Formal analysis, Conceptualization, Data curation, Project administration, Resources, Supervision, Investigation, Methodology, Validation, Visualization. **G.N. Queiroga:** Formal analysis, Methodology, Writing - review & editing. **C. Lana:** Formal analysis, Methodology. **J. Pertille:** Data curation, Writing - review & editing. **C.R.L. Michelin:** Writing - original draft, Writing - review & editing, Visualization, Supervision, Validation. **M.V.D. Remus:** Supervision, Writing - review & editing. **M.P. Roberts:** Formal analysis, Methodology. **M.P. Castro:** Formal analysis, Methodology. **C.G. Leandro:** Methodology, Software. **J.F. Savian:** Methodology, Software.

Declaration of Competing Interest

The authors declare that they have no known competing financial interests or personal relationships that could have appeared to influence the work reported in this paper.

Acknowledgements

Tiara Cerva Alves and Vitor Casagrande Dias participated in field work and sample preparation. This article is a result of the undergraduate senior thesis by Mariana Werle at Universidade Federal do Rio Grande do Sul. She held a scholarship from Conselho Nacional do

Desenvolvimento Científico e Tecnológico (CNPq) – Brazilian Government, during the investigation. Léo A. Hartmann acknowledges a research scholarship with linked grant, and overall support from CNPq. We also thank the Microscopy and Microanalysis Laboratory (LMic) of Universidade Federal de Ouro Preto, a member of FAPEMIG-supported Microscopy and Microanalysis Network of Minas Gerais, Brazil. We are grateful to Guest Editor Mathias Schannor, Ralf Halama and an anonymous reviewer that made significant contributions to the improvement of the article.

Appendix A. Supplementary data

Supplementary data to this article can be found online at https://doi.org/10.1016/j.precamres.2020.105979.

References

Abdel-Karim, A.M., Ali, S., El-Shafei, S.A., 2018. Mineral chemistry and geochemistry of ophiolitic metaultramafics from Um Halham and Fawakhir, Central Eastern Desert, Egypt. Int. J. Earth Sci. 107, 2337–2355.

Albert, C., Lana, C., Gerdes, A., Schannor, M., Narduzzia, F., Queiroga, G., 2018. Archean magmatic-hydrothermal fluid evolution in the Quadrilátero Ferrífero (SE Brazil) documented by B isotopes (LA MC-ICPMS) in tourmaline. Chem. Geol. 481, 95–109.

Amaral, L., Caxito, F.A., Pedrosa-Soares, A.C., Queiroga, G., Babinski, M., Trindade, R., Lana, C., Chemale, F., 2020. The Ribeirão da Folha ophiolite-bearing accretionary wedge (Araçuaí orogen, SE Brazil): new data for Cryogenian plagiogranite and metasedimentary rocks. Precambr. Res. 336, 105522.

Arai, S., Miura, M., 2015. Podiform chromitites do form beneath mid-ocean ridges. Lithos 232, 143–149.

Arena, K.R., Hartmann, L.A., Lana, C., 2016. Evolution of Neoproterozoic ophiolites from the southern Brasiliano Orogen revealed by zircon U-Pb-Hf isotopes and geochemistry. Precambr. Res. 285, 299–314.

Arena, K.R., Hartmann, L.A., Lana, C., 2017. Tonian emplacement of ophiolites in the southern Brasiliano Orogen delimited by U-Pb-Hf isotopes of zircon from metasomatites. Gondwana Res. 49, 296–332.

Arena, K.O., Hartmann, L.A., Lana, C., 2018. U-Pb-Hf isotopes and trace elements of metasomatic zircon delimit the evolution of the Capané ophiolite in the southern Brasiliano Orogen. Int. Geol. Rev. 60, 911–928.

Arena, K.R., Hartmann, L.A., Lana, C., Queiroga, G.N., Castro, M.P., 2020. Geochemistry and $\delta^{11}B$ evolution of tourmaline from tourmalinite as a record of oceanic crust in the Tonian Ibaré ophiolite, southern Brasiliano Orogen. Anais da Academia Brasileira de Ciências. https://doi.org/10.1590/0001-3765202020180193.

Azer, M.K., 2014. Petrological studies of Neoproterozoic serpentinized ultramafics of the Nubian Shield: spinel compositions as evidence of the tectonic evolution of Egyptian ophiolites. Acta Geol. Pol. 64 (1), 113–127.

Babinski, M., Chemale Jr., F., Hartmann, L.A., Van Schmus, W.R., Silva, L.S., 1996. Juvenile accretion at 750–700 Ma in southern Brazil. Geology 24 (5), 439–442.

Barnes, S.J., 2000. Chromite in komatiites, II. Modification during greenschist to mid-amphibolite facies metamorphism. J. Petrol. 41, 387–409.

Barnes, S.J., Roeder, P.L., 2001. The range of spinel compositions in terrestrial mafic and ultramafic rocks. J. Petrol. 42 (12), 2279–2302.

Bhat, I.M., Ahmad, T., Subba Rao, D.V., 2019. Alteration of primary Cr-spinel mineral composition from the Suru Valley ophiolitic peridotites, Ladakh Himalaya: Their low-temperature metamorphic implications. Journal of Earth System Science 128, 188 (2019). https://doi.org/10.1007/s12040-019-1222-6 128-188.

Bologna, M.S., Dragone, G.N., Muzio, R., Peel, E., Nuñez-Demarco, P., Ussami, N., 2019. Electrical structure of the lithosphere from Rio de la Plata Craton to Paraná Basin: amalgamation of cratonic and refertilized lithospheres in SW Gondwanaland. Tectonics 38, 77–94.

Boschi, C., Dini, A., Früh-Green, G.L., Kelley, D.S., 2008. Isotopic and element exchange during serpentinization and metasomatism at the Atlantis Massif (MAR 30N): insights from B and Sr isotope data. Geochim. Cosmochim. Acta 72, 1801–1823.

Brito-Neves, B.B., Fuck, R.A., Pimentel, M.M., 2014. The Brasiliano collage in South America: a review. Braz. J. Geol. 44 (3), 493–518.

Brown, M.T., Fuck, R.A., Dantas, E.L., 2020. Isotopic age constraints and geochemical results of disseminated ophiolitic assemblage from Neoproterozoic mélange, Central Brazil. Precambr. Res. 339, 105581.

Caxito, F., Uhlein, A., Stevenson, R., Uhlein, G.J., 2014. Neoproterozoic oceanic crust remnants in northeast Brazil. Geology 42, 387–390.

Cerva-Alves, T., Hartmann, L.A., Remus, M.V.D., Lana, C., 2020. Integrated ophiolite and arc evolution, southern Brasiliano Orogen. Precambr. Res. 341, 105648.

Chemale Jr., F., 2000. Evolução Geológica do Escudo Sul-rio-grandense. In: Holz, M., De Ros, L.F. (Eds.), Geologia do Rio Grande do Sul. Centro de investigação do Gondwana, Universidade Federal do Rio Grande do Sul, Porto Alegre, Brasil, pp. 13–55.

Dechamps, F., Godard, M., Guillot, S., Hattori, K., 2013. Geochemistry of subduction zone serpentinites: a review. Lithos 178, 96–127.

Derbyshire, E.J., O'Driscoll, B., Lenaz, D., Zanetti, A., Gertisser, R., 2019. Chromitite petrogenesis in the mantle section of the Ballantrae Ophiolite Complex (Scotland). Lithos 344–345, 51–67.

Dick, J.B., Bullen, T., 1984. Chromian spinel as a petrogenetic indicator in abyssal and alpine-type peridotites and spatially associated lavas. Contrib. Miner. Petrol. 86, 54–76.

Dilek, Y., 2003. Ophiolite pulses, mantle plume and orogeny. In: Dilek, Y., Robinson, P.T. (Eds.), Ophiolites in Earth History. Geological Society, London, Special Publications 218, 9-19.

Dilek, Y., Furnes, H., 2014. Ophiolites and their origins. Elements 10, 93–100.

Evans, B.W., Frost, B.R., 1975. Chrome-spinel in progressive metamorphism – a preliminary analysis. Geochim. Cosmochim. Acta 39, 959–972.

Farber, K., Dziggel, A., Trumbull, R.B., Meyer, F.M., Wiedenbeck, M., 2015. Tourmaline B-isotopes as tracers of fluid sources in silicified Palaeoarchaean oceanic crust of the Mendon Formation, Barberton greenstone belt, South Africa. Chem. Geol. 417, 134–147.

Fernandes, L.A.D., Menegat, R., Costa, A.F.U., Porcher, C.C., Tommasi, A., Kraemer, G., Ramgrab, G.E., Camozzato, E., 1995. Evolução tectônica do Cinturão Dom Feliciano no Escudo Sul-Rio-Grandense: Parte I – uma contribuição a partir do registro geológico. Revista Brasileira de Geociências 25 (4), 351–374.

Fernandes, L.A.D., Tommasi, A., Porcher, C.C., 1992. Deformation patterns in the southern Brazilian branch of the Dom Feliciano Belt: a reappraisal. J. S. Am. Earth Sci. 5, 77–96.

Garda, G.M., Trumbull, R.B., Beljavskis, P., Wiedenbeck, M., 2009. Boron isotope composition of tourmalinite and vein tourmalines associated with gold mineralization, Serra do Itaberaba Group, central Ribeira Belt, SE Brazil. Chem. Geol. 264, 207–220.

Gargiulo, M.F., Bjerg, E.A., Mogessie, A., 2013. Spinel group minerals in metamorphosed ultramafic rocks from Río de Las Tunas belt, Central Andes, Argentina. Geol. Acta 11, 133–148.

Gerdes, A., Zeh, A., 2006. Combined U-Pb and Hf isotope LA-(MC)-ICP-MS analyses of detrital zircons: comparison with SHRIMP and new constraints for the provenance and age of an Armorican metasediment in Central Germany. Earth Planet. Sci. Lett. 249, 47–61.

González-Jiménez, J.M., Kerestedjian, T., Proenza, J.A., Gervilla, F., 2009. Metamorphism on chromite ores from the Dobromirtsi Ultramafic Massif, Rhodope Mountains (SE Bulgaria). Geologica Acta 7 (4), 413–429.

González-Jiménez, J.M., Griffin, W.F., Proenza, J.A., Gervilla, F., O'Reilly, S.Y., Akbulut, M., Pearson, N.J., Arai, S., 2014. Chromitites in ophiolites: how, where, when, why? Part II. The crystallization of chromitites. Lithos 189, 140–158.

Grew, E.S., Dymek, R.F., De Hoog, J.C.M., Harley, S.L., Boak, J., Hazen, R.M., Yates, M. G., 2015. Boron isotopes in tourmaline from the ca. 3.7–3.8 Ga Isua supracrustal belt, Greenland: Sources for boron in Eoarchean continental crust and seawater. Geochim. Cosmochim. Acta 163, 156–177.

Gubert, M.L., Philipp, R.P., Basei, M.A.S., 2016. The Bossoroca Complex, São Gabriel Terrane, Dom Feliciano Belt, southernmost Brazil: U-Pb geochronology and tectonic implications for the Neoproterozoic São Gabriel Arc. J. S. Am. Earth Sci. 70, 1–17.

Hartmann, L.A., Leite, J.A.D., McNaughton, N.J., Santos, J.O.S., 1999. Deepest exposed crust of Brazil-SHRIMP establishes three events. Geology 27, 947–950.

Hartmann, L.A., Chemale Jr., F., 2003. Mid amphibolite facies metamorphism of harzburgites in the Neoproterozoic Cerro Mantiqueiras Ophiolite, southernmost Brazil. Anais Academia Brasileira de Ciências 75, 109–128.

Hartmann, L.A., Philipp, R.P., Liu, D., Wan, Y., Wang, Y., Santos, J.O.S., Vasconcellos, M. A.Z., 2004. Paleoproterozoic magmatic provenance of detrital zircons, Porongos Complex quartzites, southern Brasiliano Orogen. Int. Geol. Rev. 46, 127–157.

Hartmann, L.A., Leite, J.A.D., Silva, L.C., Remus, M.V.D., McNaughton, N.J., Groves, D.I., Fletcher, I.R., Santos, J.O.S., Vasconcellos, M.A.Z., 2000. Advances in SHRIMP geochronology and their impact on understanding the tectonic and metallogenic evolution of southern Brazil. Aust. J. Earth Sci. 47, 829–844.

Hartmann, L.A., Philipp, R.P., Santos, J.O.S., McNaughton, N.J., 2011. Time frame of the 753–680 Ma juvenile accretion during the São Gabriel orogeny, Southern Brazilian shield. Gondwana Res. 19, 84–99.

Hartmann, L.A., Vasconcellos, M.V., Bitencourt, M.F., Castro, J., Fabião, J., Monteiro, A., Pires, K., 2000. Structural and compositional evolution of Cr-spinel and hornblende, Palma Group, Rio Grande do Sul, Brazil. Revista Pesquisas em Geociências 27 (1), 15–27.

Hartmann, L.A., Werle, M., Michelin, C.R.L., Lana, C., Queiroga, G.N., Castro, M.P., Arena, K.R., 2019. Proto-Adamastor ocean crust (920 Ma) described in Brasiliano Orogen from coetaneous zircon and tourmaline. Geosci. Front. 10, 1623–1633.

Henry, D.J., Dutrow, B.L., 1996. Metamorphic tourmaline and its petrologic applications. In: Grew, E.S., Anovitz, L.M. (Ed.). Boron: Mineralogy, Petrology and Geochemistry. Reviews in Mineralogy, v. 33. Mineralogical Society of America 10, 503-557.

Hodel, F., Trindade, R.I.F., Macouin, M., Meira, V.T., Dantas, E.L., Paixão, M.A.P., Rospabé, M., Castro, M.P., Queiroga, G.N., Alkmim, A.R., Lana, C.C., 2019. A Neoproterozoic hyper-extended margin associated with Rodinia's demise and Gondwana's build-up: the Araguaia Belt, central Brazil. Gondwana Res. 66, 43–62.

Hueck, M., Oyhantçabal, P., Philipp, R.P., Basei, M.A.S., Siegesmund, S., 2018. The Dom Feliciano belt in Southern Brazil and Uruguay. In: Siegesmund, S., Basei, M.A.S., Oyhantçabal, P., Oriolo, S. (Eds.), Geology of Southwest Gondwana. Regional Geology Reviews, Springer Nature, pp. 243–265.

Irvine, T.N., 1967. Chromian spinel as a petrogenetic indicator. Part 2. Petrologic applications. Can. J. Earth Sci. 4, 71–103.

Ismalil, S.A., 2009. Chemistry of accessory chromian spinel in serpentinites from the Penjwen ophiolite rocks, Zagros thrust zone, northeastern Iraq. J. Kirkuk Univ. – Scientific Studies 4, 1–21.

Jost, H., Hartmann, L.A., 1979. Rodingitos do Rio Grande do Sul, Brasil. Acta Geologica Leopoldensia 3, 77–91.

Kimball, K.L., 1990. Effects of hydrothermal alteration on the compositions of chromian spinels. Contrib. Miner. Petrol. 105, 337–346.

Konopásek, J., Cavalcante, C., Fossen, H., Janousec, V., 2020. Adamastor – an ocean that never existed? Earth-Sci. Rev. 205, 103201.
Kotschoubey, B., Hieronymus, B., Albuquerque, C.A.R., 2005. Disrupted peridotites and basalts from the Neoproterozoic Araguaia belt (northern Brazil): remnants of a poorly evolved oceanic crust? J. South Am. Earth Sci. 20, 211–230.
Leite, J.A.D., Hartmann, L.A., McNaughton, N.J., Chemale Jr., F., 1998. SHRIMP U/Pb zircon geochronology of Neoproterozoic juvenile and crustal-reworked terranes in southernmost Brazil. Int. Geol. Rev. 40, 688–705.
Lopes, C.G., Pimentel, M.M., Philipp, R.P., Gruber, L., Armstrong, R., Junges, S., 2015. Provenance of the Passo Feio complex, Dom Feliciano Belt: implications for the age of supracrustal rocks of the São Gabriel Arc, Southern Brazil. J. S. Am. Earth Sci. 58, 9–17.
Marques, J.C., 1996. Petrologia e metalogênese da sequência metaultramáfica da Antiforme Capané, Suíte metamórfica Porongos, Cachoeira do Sul – RS. 246 pp. MSc thesis. Universidade Federal do Rio Grande do Sul, Porto Alegre.
Marques, J.C., Roisenberg, A., Jost, H., Frantz, J.C., Teixeira, R.S., 2003. Geologia e geoquímica das rochas metaultramáficas da Antiforme Capané, Suíte Metamórfica Porongos, RS. Revista Brasileira Geociências 33, 95–107.
Marschall, H.R., Ludwig, T., Altherr, R., Kalt, A., Tonarini, S., 2006. Syros metasomatic tourmaline: evidence for very high-δ^{11}B fluids in subduction zones. J. Petrol. 47 (10), 1915–1942.
Marschall, H.R., 2018. Boron isotopes in the ocean floor realm and the mantle. In: Marschall, H.R., Foster, G.L. (Eds.), Boron Isotopes, Advances in Isotope Geochemistry. Springer International Publishing AG. https://doi.org/10.1007/978-3-319-64666-4_8.
Marschall, H.R., Foster, G.L., 2018. Boron Isotopes in the Earth and Planetary Sciences – A Short History and Introduction. In: Marschall, H.R., Foster, G.L. (Eds.) Boron Isotopes, Advances in Isotope Geochemistry. Springer International Publishing AG 2018. https://doi.org/10.1007/978-3-319-64666-4_1.
Massuda, A.J., Hartmann, L.A., Queiroga, G.N., Castro, M.P., Leandro, C.G., Savian, J.F., 2020. Mineralogical evolution of the northern Bossoroca ophiolite, São Gabriel terrane. Brazilian. J. Geol. https://doi.org/10.1590/2317-4889202020190120.
Miura, M., Arai, S., Ahmed, A.H., Mizukami, T., Okuno, M., Yamamoto, S., 2012. Podiform chromitite classification revisited: a comparison of discordant and concordant chromitite pods from Wadi Hilti, northern Oman ophiolite. J. Asian Earth Sci. 59, 52–61.
Mohanty, N., Singh, S.P., Satyanarayanan, M., Jayananda, M., Korakoppa, M.M., Hiloidari, S., 2018. Chromian spinel compositions from Madawara ultramafics, Bundelkhand Craton: implications on petrogenesis and tectonic evolution of the southern part of Bundelkhand Craton, Central India. Geol. J. 2018, 1–25.
Paim, P.S.G., Chemale Jr., F., Wildner, W., 2014. Estágios evolutivos da Bacia do Camaquã. Ciência e Natura 36, 183–193.
Parkinson, I.J., Pearce, J.A., 1998. Peridotites from the Izu–Bonin–Mariana Forearc (ODP Leg 125): Evidence for Mantle Melting and Melt-Mantle Interaction in a Supra-Subduction Zone Setting. J. Petrol. 39 (9), 1577–1618.
Peel, E., Bettucci, L.S., Basei, M.A.S., 2018. Geology and geochronology of Paso del Dragón Complex (northeastern Uruguay): implications on the evolution of the Dom Feliciano Belt (Western Gondwana). J. S. Am. Earth Sci. 85, 250–262.
Pertille, J., Hartmann, L.A., Philipp, R.P., 2015. Zircon U-Pb age contrains the Paleoproterozoic sedimentary basement of the Ediacaran Porongos Group, Sul-Riograndense Shield, southern Brazil. J. S. Am. Earth Sci. 63, 334–345.
Pertille, J., Hartmann, L.A., Philipp, R.P., Petry, T.S., Lana, C.C., 2015. Origin of the Ediacaran Porongos Group, Dom Feliciano Belt, southern Brazilian Shield, with emphasis on whole rock and detrital zircon geochemistry and U-Pb, Lu-Hf isotopes. J. S. Am. Earth Sci. 64, 69–93.
Pertille, J., Hartmann, L.A., Santos, J.O.S., McNaughton, N.J., Armstrong, R., 2017. Reconstructing the Cryogenian-Ediacaran evolution of the Porongos fold and thrust Belt, southern Brasiliano Orogen, based on zircon U-Pb-Hf-O isotopes. Int. Geol. Rev. 59, 1532–1560.
Philipp, R.P., Machado, R., 2005. The late Neoproterozoic granitoid magmatism of the Pelotas Batholith, southern Brazil. J. S. Am. Earth Sci. 19, 461–478.
Philipp, R.P., Pimentel, M.M., Chemale Jr., F., 2016. Tectonic evolution of the Dom Feliciano Belt in Southern Brazil: geological relationships and U-Pb geochronology. Braz. J. Geol. 46, 83–104.
Philipp, R.P., Pimentel, M.M., Basei, M.A.S., 2018. The tectonic evolution of the São Gabriel Terrane, Dom Feliciano Belt, southern Brasil: the closure of the Charrua Ocean. In: Siegesmund, S., Basei, M.A.S., Oyhantçabal, P., Oriolo, S. (Eds.), Gology of Southwest Gondwana. Regional Geology Reviews, Springer Nature, pp. 243–265.
Qiu, T., Zhu, Y., 2018. Chromian spinels in highly altered ultramafic rocks from the Sartohay ophiolitic mélange, Xinjiang, NW China. J. Asian Earth Sci. 159, 155–184.
Ramos, R.C., Koester, E., Porcher, C.C., 2017. Chemistry of chromites from Arroio Grande Ophiolite (Dom Feliciano Belt, Brazil) and their possible connection with the Nama Group (Namibia). J. S. Am. Earth Sci. 80, 192–206.
Ramos, R.C., Koester, E., Vieira, D.T., 2020. Sm–Nd systematics of metaultramafic-mafic rocks from the Arroio Grande Ophiolite (Brazil): insights on the evolution of the South Adamastor paleo-ocean. Geosci. Front. https://doi.org/10.1016/j.gsf.2020.02.013.
Rapela, C.W., Fanning, C.M., Casquet, C., Pankhusrt, R.J., Spalletti, L., Poiré, D., Baldo, E.G., 2011. The Rio de la Plata craton and the adjoining Pan African/Brasiliano terranes: their origins and incorporation into south-west Gondwana. Gondwana Res. 20, 673–690.
Remus, M.V.D., McNaughton, N.J., Hartmann, L.A., Koppe, J.C., Fletcher, I.R., Groves, D. I., Pinto, V.M., 1999. Gold in the Neoproterozoic juvenile Bossoroca Volcanic Arc of southernmost Brazil: isotopic constraints on timing and sources. J. S. Am. Earth Sci. 12, 349–366.
Rizeli, M.E., Beyarslan, M., Wang, K., Bingöl, A.F., 2016. Mineral chemistry and petrology of mantle peridotites from the Guleman ophiolite (SE Anatolia, Turkey): evidence of a forearc setting. J. Afr. Earth Sc. 123, 392–402.
Rollinson, H., 2008. The geochemistry of mantle chromitites from the northern part of the Oman ophiolite: inferred parental melt compositions. Contrib. Mineral. Petrol. 156, 273–288.
Saalmann, K., Hartmann, L.A., Remus, M.V.D., Koester, E., Conceição, R.V., 2005. Sm-Nd isotope geochemistry of metamorphic volcano-sedimentary successions in the São Gabriel Block, southernmost Brazil: evidence for the existence of juvenile Neoproterozoic ocean crust to the east of the Rio de la Plata craton. Precambr. Res. 136, 159–175.
Saalmann, K., Remus, M.V.D., Hartmann, L.A., 2007. Neoproterozoic magmatic arc assembly in the southern Brazilian Shield – constraints for a plate tectonic model for the Brasiliano orogeny. Geotectonic Res. 95, 41–59.
Saalmann, K., Gerdes, A., Lahaye, Y., Hartmann, L.A., Remus, M.V.D., Laufer, A., 2011. Multiple accretion at the eastern margin of the Rio de la Plata craton: the prolonged Brasiliano orogeny in southernmost Brazil. Int. J. Earth Sci. 100, 355–378.
Saccani, E., Samuel, V., Santosh, M., 2020. Ophiolites – Geodynamic and environmental implications: preface. Geosci. Front. 11 (1), 1–2.
Schannor, M., Lana, C., Fonseca, M.A., 2019. São Francisco-Congo Craton break-up delimited by U-Pb-Hf isotopes and trace-elements of zircon from metasediments of the Araçuaí Belt. Geosci. Front. 10, 611–628.
Silva, L.C., McNaughton, N.J., Armstrong, R., Hartmann, L.A., Fletcher, I.R., 2005. The neoproterozoic Mantiqueira Province and its African connections: a zircon-based U-Pb geochronologic subdivision for the Brasiliano/Pan-African systems of orogens. Precambr. Res. 136, 203–240.
Stern, R.J., Johnson, P.R., Kröner, A., Yibas, B., 2004. Neoproterozoic ophiolites of the Arabian-Nubian shield. In: Kusky, T.M. (Ed). Precambrian Ophiolites and Related Rocks. Developments in Precambrian Geology 13, 95-128.
Suita, M.T.F., Strieder, A.J., 1996. Cr-Spinels from Brazilian mafic-ultramafic complexes: metamorphic modifications. Int. Geol. Rev. 38, 245–267.
Suita, M.T.F., Pedrosa-Soares, A.C., Leite, C.A.A., Nilson, A.A., Prichard, H.M., 2004. Complexos ofiolíticos do Brasil e a metalogenia comparada das faixas Araçuaí e Brasília. In: Pereira, E., Castroviejo, R., Ortiz, F. (Eds.), Complejos Ofiolíticos em Iberoamérica: guías de prospección para metales preciosos. Rede CYTED, pp. 101-132.
Trumbull, R.B., Beurlen, H., Wiedenbeck, M., Soares, D.R., 2013. The diversity of B-isotope variations in tourmaline from rare-element pegmatites in the Borborema Province of Brazil. Chem. Geol. 352, 47–62.
Trumbull, R.B., Slack, J.F., 2018. Boron isotopes in the continental crust: granites, pegmatites, felsic volcanic rocks, and related ore deposits. In: Marschall, H.R., Foster, G.L. (Eds.) Boron Isotopes, Advances in Isotope Geochemistry. Springer International Publishing AG 2018. https://doi.org/10.1007/978-3-319-64666-4_1.
Van Hinsberg, V.J., Henry, D.J., Marschall, H.R., 2011. Tourmaline: an ideal indicator of its host environment. Canad. Mineral. 49, 1–16.
Vedana, L.A., Philipp, R.P., Basei, M.A.S., 2017. Tonian to early Cryogenian synorogenic basin of the São Gabriel Terrane, Dom Feliciano Belt, southernmost Brazil. Int. Geol. Rev. 60 (1), 109–133.
Warren, J.M., 2016. Global variations in abyssal peridotites compositions. Lithos 248–251, 193–219.
Werle, M., Hartmann, L.A., Michelin, C.R.L., Lana, C., Queiroga, G.N., Arena, K.R., 2019. Tonian oceanic crust processes decoded with multi-techniques from metamorphosed, hydrothermal, coetaneous zircon-tourmaline, southern Brasiliano Orogen. Geophysical Research Abstracts 21, EGU2019 – 1048.
Whitney, D.L., Evans, B.W., 2010. Abbreviations for names of rock-forming minerals. Am. Mineral. 95, 185–187.
Xavier, K.F., Oshiro, Y.M., Pinto, V.M., Hartmann, L.A., Fragoso, B. 2019. Variação composicional da cromita e implicações tectônicas na evolução do ofiolito Candiotinha, sul do Escudo Brasileiro. Anais do XVII Simpósio Nacional de Estudos Tectônicos, Bento Gonçalves, RS, p. 317.
Yamaoka, K., Matsukura, S., Ishikawa, T., Kawahata, H., 2015. Boron isotope systematics of a fossil hydrothermal system from the Troodos ophiolite, Cyprus: water–rock interactions in the oceanic crust and subseafloor ore deposits. Chem. Geol. 396, 61–73.
Zhou, M.F., Robinson, P.T., Malpas, J., Aitchison, J., Sun, M., Bai, W.J., Hu, X.F., Yang, J. S., 2001. Melt/mantle interaction and melt evolution in the Sartohay high-Al chromite deposits of the Dalabute ophiolite (NW China). J. Asian Earth Sci. 19, 517–534.
Zvirtes, G., Philipp, R.P., Camozzato, E., Guadagnin, F., 2017. Análise estrutural do Metagranito Capané, Complexo Porongos, Cachoeira do Sul. RS. Revista Pesquisas em Geociências 44 (1), 5–23.